Sulfoquinovose is exclusively metabolized by the gut microbiota and degraded differently in mice and humans

Julia Krasenbrink[1,2], Buck T. Hanson[1,3], Anna S. Weiss[4§], Sabrina Borusak[5,6], Tomohisa Sebastian Tanabe[1], Michaela Lang[1], Georg Aichinger[7,8], Bela Hausmann[9,10], David Berry[1,9], Andreas Richter[11], Doris Marko[7], Marc Mussmann[1], David Schleheck[5,6], Bärbel Stecher[4,12,13], Alexander Loy[1,9]*

[1] University of Vienna, Centre for Microbiology and Environmental Systems Science, Division of Microbial Ecology, Vienna, Austria
[2] University of Vienna, Doctoral School in Microbiology and Environmental Science, Vienna, Austria
[3] Bioscience Division, Los Alamos National Laboratory, Los Alamos, New Mexico, USA
[4] Max von Pettenkofer Institute of Hygiene and Medical Microbiology, Faculty of Medicine, Ludwig Maximilian University, Munich, Germany
[5] Department of Biology, University of Konstanz, Konstanz, Germany
[6] Konstanz Research School Chemical Biology, University of Konstanz, Konstanz, Germany
[7] Department of Food Chemistry and Toxicology, University of Vienna, Austria
[8] Department of Health Sciences and Technology, ETH Zurich, Switzerland
[9] Joint Microbiome Facility of the Medical University of Vienna and the University of Vienna, Vienna, Austria
[10] Division of Clinical Microbiology, Department of Laboratory Medicine, Medical University of Vienna, Vienna, Austria
[11] University of Vienna, Centre for Microbiology and Environmental Systems Science, Division of Terrestrial Ecosystem Research, Vienna, Austria
[12] German Center for Infection Research (DZIF), Partner Site Munich, Munich, Germany
[13] Chair of Intestinal Microbiome, School of Life Sciences, Technical University of Munich, Germany

*Corresponding author: Alexander Loy alexander.loy@univie.ac.at

[§]Current affiliation:
Anna S. Weiss, Microbial Systems Ecology Group, Institute of Biogeochemistry and Pollutant Dynamics, Department of Environmental Systems Sciences, ETH Zurich, Zurich, Switzerland

Abstract

Background

Sulfoquinovose (SQ) is a green-diet-derived sulfonated glucose and a selective substrate for few human gut bacteria. Complete anaerobic SQ degradation via interspecies metabolite transfer to sulfonate-respiring bacteria produces hydrogen sulfide, which has dose- and context-dependent health effects. Here, we studied potential SQ degradation by the mammalian host and the impact of SQ supplementation on human and murine gut microbiota diversity and metabolism.

Results

$^{13}CO_2$ breath tests with germ-free C57BL/6 mice gavaged with ^{13}C-SQ were negative. Also, SQ was not degraded by human intestinal cells *in vitro*, indicating that SQ is not directly metabolized by mice and humans. Addition of increasing SQ concentrations to human fecal microcosms revealed dose-dependent responses of the microbiota and corroborated the relevance of *Agathobacter rectalis* and *Bilophila wadsworthia* in cooperative degradation of SQ to hydrogen sulfide via interspecies transfer of 2,3-dihydroxy-1-propanesulfonate (DHPS). Similar to the human gut microbiome, the genetic capacity for SQ or DHPS degradation is sparsely distributed among bacterial species in the mouse gut. *Escherichia coli* and *Enterocloster clostridioformis* were identified as primary SQ degraders in the mouse gut. SQ and DHPS supplementation experiments with conventional laboratory mice and their intestinal contents showed that SQ was incompletely catabolized to DHPS. Although some *E. clostridioformis* genomes encode an extended sulfoglycolytic pathway for both SQ and DHPS fermentation, SQ was only degraded to DHPS by a mouse-derived *E. clostridioformis* strain.

Conclusions

Our findings suggest that SQ is solely a nutrient for the gut microbiota and not for mice and humans, emphasizing its potential as a prebiotic. SQ degradation by the microbiota of conventional laboratory mice differs from the human gut microbiota by absence of DHPS degradation activity. Hence, the microbiota of conventional laboratory mice does not fully represent the SQ metabolism in humans, indicating the need for alternative model systems to assess the impact of SQ on human health. This study advances our understanding of how individual dietary compounds shape the microbial community structure and metabolism in the gut and thereby potentially influence host health.

Key words

Sulfoquinovose, prebiotic, hydrogen sulfide, organosulfonate, sulfur metabolism, gut microbiome

Introduction

The sulfonated glucose sulfoquinovose (6-deoxy-6-sulfo-D-glucose, SQ) is an abundant sulfur molecule in the global sulfur cycle. As the polar headgroup of the sulfonolipid sulfoquinovosyldiacylglycerol (SQDG), an estimated 10 billion tons of SQ is synthesized annually by photosynthetic organisms such as plants, algae, and cyanobacteria [1]. SQDG is located in thylakoid membranes and maintains the activity and structural integrity of photosystem II [2–5]. Sulfoglycolytic microorganisms can cleave SQ from SQDG or other SQ glycosides via a sulfoquinovosidase. Two types of sulfoquinovosidase enzymes are known.

82 The YihQ sulfoquinovosidase belongs to glycoside hydrolase family 31 [6] and the NAD^+-
83 dependent SqgA sulfoquinovosidase belongs to glycoside hydrolase family 188 [7]. To date,
84 six microbial SQ degradation pathways have been described. In two pathways, SQ is
85 catabolized aerobically to sulfite by individual organisms using an alkanesulfonate
86 monooxygenase [8] or an iron- and alpha-ketoglutarate-dependent alkanesulfonate
87 dioxygenase [9]. The other pathways require syntrophic interspecies metabolite transfer of
88 C_2- or C_3-organosulfonates for complete degradation. The sulfo-Embden-Meyerhof-Parnas
89 pathway generates the C_3-organosulfonates 2,3-dihydroxypropane-1-sulfonate (DHPS) or 3-
90 sulfolactate (SL) during aerobic or anaerobic growth [10,11]. The sulfo-Entner-Doudoroff-
91 pathway degrades SQ aerobically to SL [12]. The sulfofructose-transaldolase pathway
92 produces SL aerobically and SL or DHPS anaerobically [13,14]. The sulfo-transketolase
93 pathway degrades SQ to two molecules of the C_2-organosulfonates isethionate or, putatively,
94 sulfoacetate [11]. In these pathways, the residual carbon skeleton (either C_3 or C_2) enters the
95 central carbon metabolism while organosulfonates are excreted.
96
97 DHPS is a key metabolite of SQ-degrading human gut bacteria (Figure 1 a) [15]. Four pathways
98 for anaerobic DHPS degradation are currently known (Figure 1 b). Two of these pathways are
99 utilized by select sulfite-reducing bacteria (*Desulfovibrio*, *Bilophila*) and result in the
100 intracellular formation of sulfite, which is subsequently respired to hydrogen sulfide (H_2S). In
101 *Desulfovibrio* strain DF1, DHPS is degraded to pyruvate and sulfite via 3-sulfolactaldehyde and
102 SL [16]. In *Bilophila wadsworthia*, DHPS is cleaved to hydroxyacetone and sulfite [15,17].
103 Some fermenting bacteria, such as *Klebsiella oxytoca* and *Hungatella hathewayi*, can degrade
104 DHPS by reducing it to 3-hydroxypropane-1-sulfonate (3-HPS) via sulfopropionaldehyde in a
105 third pathway [17]. In a fourth, bifurcated pathway in *Enterococcus gilvus*, DHPS is converted

to both 3-HPS and 3-sulfopropionate [18]. In the human gut, *B. wadsworthia* may use 3-sulfopropionate, but not 3-HPS, as a terminal electron acceptor resulting again in H_2S formation [18]. The strictly anaerobic mouse gut bacterium *Taurinivorans muris* encodes another potential DHPS degradation pathway, but did not degrade DHPS in growth tests [19]. However, this pathway was thus far only demonstrated in aerobic bacteria, which have the sulfopropanediol-3-dehydrogenase HpsN to oxidize (*R*)-DHPS to (*R*)-sulfolactate [20], which is then cleaved to pyruvate and sulfite by sulfolactate-sulfolyase SuyAB [21].

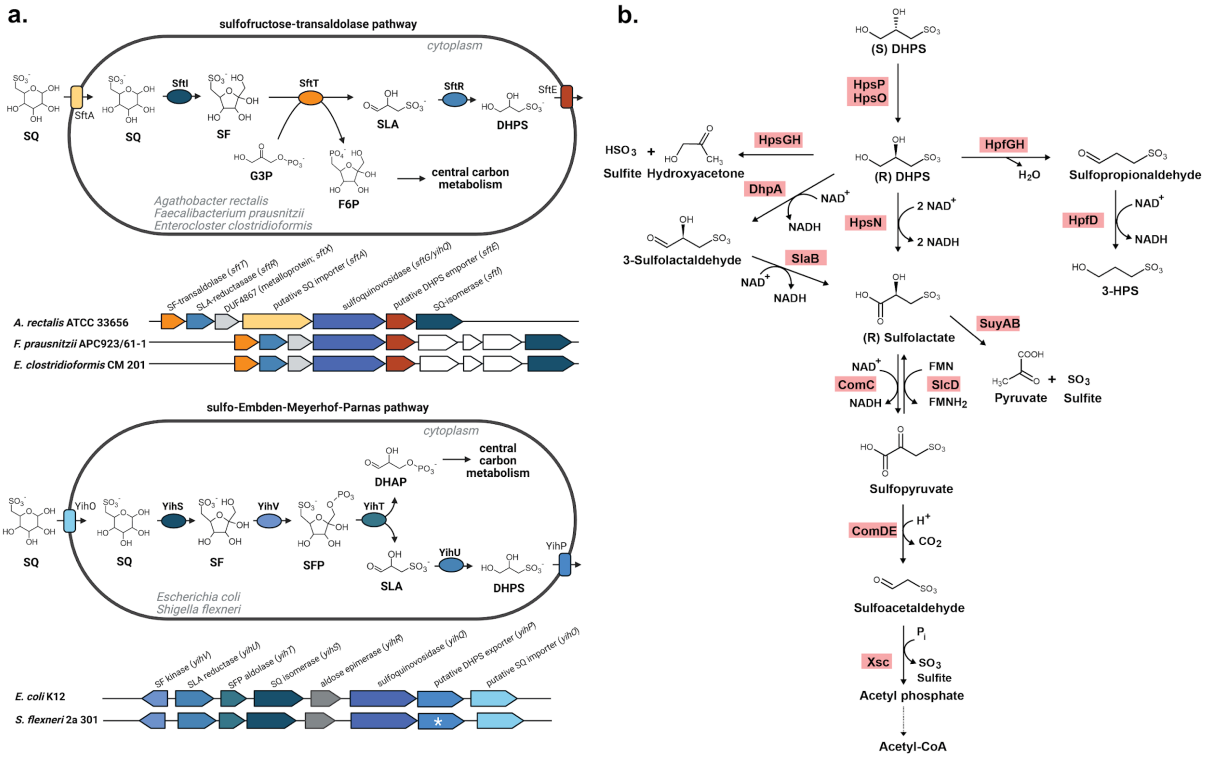

Figure 1: Prevalent SQ degradation pathways in the human gut and overview of enzymatic DHPS degradation reactions. SQ is degraded to DHPS via the sulfofructose-transaldolase pathway in *Agathobacter rectalis* (GCF_000020605.1), *Faecalibacterium prausnitzii* (GCF_003287495.1), and *Enterocloster clostridioformis* (GCF_000371405.1) or via the sulfo-Embden-Meyerhof-Parnas pathway in *Escherichia coli* (GCF_000005845.2) and *Shigella flexneri* (GCF_000006925.2) (created with biorender.com) (a). Genes depicted in white have no predicted function. The white asterisk indicates that the *yihP* homolog of *S. flexneri* contains a frameshift and is thus a potential pseudogene. Overview of known DHPS degradation pathways (b). HpsP, DHPS-2-dehydrogenase; HpsO, DHPS-2-dehydrogenase; HpsG, DHPS-sulfolyase; HpsH, DHPS-sulfolyase activating enzyme; HpfG, DHPS-dehydratase; HpfH, DHPS-dehydratase activating enzyme; HpfD, sulfopropionaldehyde reductase; HpsN, DHPS-1-dehydrogenase; DhpA, dehydrogenase; SlaB, dehydrogenase; SuyAB sulfolactate-sulfolyase; ComC, sulfolactate dehydrogenase; SlcD, sulfolactate dehydrogenase; ComDE, 3-sulfopyruvate decarboxylase; Xsc, sulfoacetaldehyde acetyltransferase. SQ, sulfoquinovose; SF, 6-deoxy-6-sulfofructose; SLA, 3-sulfolactaldehyde; DHPS, 2,3-dihydoxypropane-1-sulfonate; G3P, glycerinaldehyde-3-phosphate; F6P, fructose-6-phosphate; SFP, 6-deoxy-6-sulfofructose phosphate; DHAP, dihydroxyacetone phosphate.

As a component of edible green plants and algae, SQDG is part of the human and animal diet. While the capability of mammalian cells to metabolize SQ remains unclear, SQ is a selective

129 substrate for a few but abundant human gut bacteria [15]. *Agathobacter rectalis* (formerly
130 *Eubacterium rectale*) and *B. wadsworthia* were identified as main primary and secondary SQ
131 degraders in human fecal microcosms, respectively. Nearly half of the high-quality *A. rectalis*
132 genomes from a human microbiome database [22] encoded SQ degradation via the
133 sulfofructose-transaldolase pathway, though this potential was rare among other human gut
134 bacteria, with only 0.5% of species-level genome bins containing the pathway. Despite its
135 limited genomic prevalence, the sulfofructose-transaldolase pathway ranked among the top
136 third most abundant microbial pathways in fecal metatranscriptome datasets of four human
137 cohorts. This highlights SQ degradation as a core function of the human gut microbiome, with
138 *A. rectalis* and *Faecalibacterium prausnitzii* contributing most to its transcription [15]. Primary
139 SQ degraders are generally associated with beneficial host effects [23,24] and thus SQ is a
140 candidate prebiotic. However, excessive stimulation of secondary, H_2S-producing SQ
141 degraders may be harmful as H_2S has dose-dependent impacts on host health [25]. At low
142 nano- to micromolar concentrations, H_2S has predominantly beneficial effects [26]. H_2S serves
143 as an energy source for mitochondria, as a cellular antioxidant, and as a gasotransmitter in
144 mammals [27]. Additionally, H_2S may prevent colonization by pathogens by inhibiting their
145 aerobic respiration [28]. At high micro- to millimolar concentrations produced by the gut
146 microbiota [26], however, H_2S may disrupt disulfide bonds in the intestinal mucosal layer,
147 thus enabling bacterial penetration [29], and can lead to cell death by inhibiting cytochrome
148 *c* [30]. Overabundance of H_2S-producing bacteria, such as *B. wadsworthia*, is considered as a
149 potential driver of gut inflammation [29,31,32].
150
151 Here, we assessed the prebiotic potential of SQ by studying its degradation and metabolism
152 in humans and mice using both human and mouse gut content microcosm experiments, as

153 well as *in vivo* interventions in conventional and germ-free mice. We elucidated the role of
154 mammalian cells in SQ metabolism through *in vitro* cultures and stable isotope-tracing in
155 germ-free mice. We show that SQ is not degraded by the host, establish a minimum SQ
156 concentration that impacts the human gut microbiota, and uncover fundamental differences
157 in the bacterial SQ metabolism between wild type mice and humans.
158

159 # Materials and Methods

160 ## Human cell culture

161 HT-29, a human colorectal adenocarcinoma cell line (German Collection of Microorganisms
162 and Cell Cultures, Germany), was cultured in Dulbecco's Modified Eagles Medium (DMEM),
163 which contains 25 mM glucose, supplemented with 10% (v/v) fetal calf serum and 1% (v/v)
164 penicillin/streptomycin at 37°C and 5% CO_2 under humidified conditions. All components
165 were purchased from Invitrogen™ Life Technologies (Germany). Cells were regularly
166 monitored for mycoplasma contamination.
167 To investigate whether human intestinal cells degrade SQ, HT-29 cells were grown in DMEM
168 or in glucose-free DMEM either supplemented with 25 mM glucose, 25 mM SQ, or left
169 unamended. Supernatants were sampled after 0, 1, 6, 24, and 48 h and stored at -20°C for
170 metabolite analysis by capillary electrophoresis.
171 To study the potential inhibitory effect of SQ on the growth of HT-29 cells, 7,500 cells were
172 seeded per well and incubated in DMEM medium supplemented with glucose or SQ at three
173 concentrations (2.5 mM, 25 mM, 250 mM). In three independent experiments, duplicate
174 incubations (n = 6) were performed for all treatments. Protein production was measured as a
175 proxy for growth after 3, 5, and 7 days of incubation using sulforhodamine B colorimetric

176 assays as described previously [33]. Briefly, plates were washed with 1x PBS twice and cells
177 were fixed with a 5% trichloroacetic acid solution. Plates were dried overnight at room
178 temperature. Then, the plates were stained with 0.4% (w/v) sulforhodamine B for 1 h. After
179 washing twice with water and twice with 1% (v/v) acetic acid, the stain was eluted using a 10
180 mM Tris buffer (pH 10). Absorbance was measured at 570 nm and normalized to the solvent
181 control (1% v/v DMSO) to assess the impact of treatments on cell growth.
182

183 **Germ-free mouse experiment and $^{13}CO_2$ breath test**

184 Six germ-free male C57BL/6 mice (6–20 weeks old), were housed under sterile conditions in
185 flexible film isolators (North Kent Plastic Cages, England) or in Han-gnotocages (ZOONLAB
186 GmbH, Germany). Mice were kept on a twelve-hour light-dark cycle at 20.5-23.5°C and 45-
187 65% humidity, with autoclaved water and Mouse-Breeding complete feed (Ssniff, Germany)
188 provided *ad libitum*. Mice were scored twice daily for their health status, and sterility was
189 checked monthly during housing, before the experiment, and during the experiment using
190 qPCR with universal bacterial 16S rRNA gene primers [34,35]. Mice were randomly assigned
191 to two treatment groups and kept in separate cages. The administered substrates were either
192 10 mg of fully ^{13}C-labeled D-glucose (Sigma-Aldrich, Germany) or 10 mg of fully ^{13}C-labeled
193 SQ, which was synthesized from fully ^{13}C-labeled D-glucose following an established protocol
194 [36]. Each treatment group received their substrate dissolved in 100 µl sterile water
195 (Ampuwa; Fresenius Kabi, Germany) via gavage. Respired air from individual mice was
196 sampled for CO_2 stable isotope analysis prior to gavage (baseline) and at 1, 3, 6, 9, 12, and 24
197 h post-gavage. For breath air sampling, individual mice were placed in an airtight one-liter
198 container sealed with a lid fitted with a rubber stopper for approximately 2 minutes. Separate

199 containers were used for each treatment group to avoid cross-contamination between
200 groups. Gas samples (15 ml) were taken at 30 and 90 seconds and injected entirely into pre-
201 vacuumed exetainers (12 ml) creating an overpressure to prevent leakage from ambient air
202 into the exetainers. Ambient air samples were taken before the experiment for blank
203 measurements. If feasible, fecal samples were collected to validate sterility of mice and for
204 metabolite analysis. $^{13}CO_2$ concentrations were measured in the gas samples using isotope
205 ratio mass spectrometry (GasBench II headspace sampler connected to a Delta V Advantage
206 isotope mass spectrometer; Thermo Fisher Scientific, Germany). $^{13}CO_2$ production rates per
207 minute were calculated from the differences in $^{13}CO_2$ (atom percent excess) between the two
208 samples taken at 30 s and 90 s.
209

210 Anoxic *in vitro* gut microcosm incubations and pure culture growth tests

211 All anoxic incubations and growth tests were performed in an anaerobic tent (Coy Laboratory
212 Products, United States) operated with a gas mix of 85% N_2, 10% CO_2 and 5% H_2. The H_2 levels
213 in the tent atmosphere ranged between 1.5 and 2.5%.
214 Fecal samples were collected from five human individuals, who had not taken antibiotics in
215 the three months before sampling. Samples were stored at 4°C for maximally 24 h before
216 processing. All samples were pooled, and 3.9 g of fecal mass was homogenized in oxygen-free
217 30 mM bicarbonate buffer (pH 6.8). This fecal slurry (1.32 mg/ml) was distributed into 20 ml
218 Hungate tubes (final volume: 15 ml) and sealed with butyl-rubber stoppers and screw-on
219 caps. Triplicate microcosms were amended with 10 mM, 1 mM, 0.1 mM, or 0.01 mM SQ
220 (MCAT GmbH, Germany). One microcosm was left unamended (negative control). Tubes were
221 incubated at 37°C and subsamples (1 ml) were collected after 0, 3, 6, 9, 12, 16, and 24 h. From

222 each subsample, 20 µl was used for sulfide quantification. The remaining subsample was
223 centrifuged at 11,000 x g for 5 min at 4°C. Biomass-free supernatants were stored at -20°C for
224 subsequent capillary electrophoresis. Cell pellets were frozen at -80°C for DNA extraction.
225
226 In two independent experiments, we sampled intestinal contents of conventional C57BL/6
227 wild type mice to create mouse gut content slurries. Mice were housed under specific-
228 pathogen-free conditions with standard chow diet (Ssniff V1534, Ssniff, Germany) and water
229 *ad libitum*, in compliance with Federation of European Laboratory Animal Science
230 Associations guidelines [37]. Specific pathogen-free status was confirmed through regular
231 screening for viral, bacterial, mycoplasmal, and parasitic agents such as murine norovirus,
232 mouse hepatitis virus, *Helicobacter* species, *Salmonella* species, *Streptococcus* species,
233 protozoa, and helminths. After euthanasia, mice were dissected in an anaerobic chamber.
234 In the first experiment, ten mice (4 females, 6 males, 8–10 weeks old) were dissected, and
235 their small intestinal, cecal and large intestinal contents were pooled and homogenized with
236 oxygen-free 1x PBS (pH 7.4). The gut content slurry (5.25 mg/ml) was distributed into 20 ml
237 Hungate tubes (final volume: 10 ml). Mouse gut microcosms were left unamended or
238 amended with 10 mM SQ or 10 mM DHPS. All treatments were performed in triplicate.
239 Hungate tubes were sealed with butyl-rubber stoppers and screw-on caps and incubated at
240 37°C. Subsamples were collected at 0, 24, 48, and 96 h, and sulfide was quantified in 20 µl of
241 subsample.
242 In the second experiment, eight mice (4 females, 4 males, 8–10 weeks old) were dissected,
243 and their small intestinal (2.2 g) and cecal contents (5.9 g) were separately pooled. Small
244 intestine and cecal contents were homogenized with oxygen-free 1x PBS (pH 7.4) and
245 transferred into 20 ml Hungate tubes (final volume: 15 ml) with a concentration of 4.9 mg/ml

246 and 5.15 mg/ml of small intestinal and cecal content, respectively. Both sets of microcosms
247 were left unamended or amended with 10 mM SQ, and sealed with butyl-rubber stoppers
248 and screw-on lids for incubation at 37°C. All treatments were performed in triplicate.
249 Subsamples (1 ml) were taken at 0, 24, 120, and 220 h. In both experiments, subsamples were
250 centrifuged at 11,000 x g for 5 min at 4°C. Pellets were stored for DNA extraction at -80°C and
251 biomass-free supernatants were stored at -20°C for metabolite analyses.
252
253 *Enterocloster clostridioformis* YL32 (DSM 26114) and *Faecalibaculum rodentium* ALO17 (DSM
254 103405) were each grown in triplicate cultures in 100% and 30% brain heart infusion broth
255 with or without 10 mM SQ at 37°C in gas-tight Hungate tubes. Anoxic and autoclaved
256 ultrapure water was used for dilution of the medium. Growth was monitored by measuring
257 optical density at 600 nm. Identities of grown strains were confirmed by direct Sanger
258 sequencing (Microsynth GmbH, Austria) of 16S rRNA gene amplicons.
259

260 **Conventional wild type mouse experiment**

261 Fifteen conventional C57BL/6 wild type mice (6-8 weeks) were bred and housed under specific
262 pathogen-free conditions in accordance with the guidelines of the Federation of European
263 Laboratory Animal Science Associations [37]. As aforementioned, specific pathogen-free
264 status was confirmed through regular screening. Mice were maintained with *ad libitum* water
265 and autoclaved mouse chow (Ssniff V1534, Ssniff, Germany). The day/night cycle was 14/10
266 hours, and environmental conditions were maintained at 20–24°C with 45–65% humidity.
267 After one week of acclimatization, mice were randomly assigned to three groups (two males
268 and three females each) with no significant differences in weight between groups. Two

269 treatment groups were gavaged with 1 mg or 10 mg SQ in 100 µl aqueous solutions, while the
270 third, control group was gavaged with 100 µl autoclaved tap water. Fecal samples were
271 collected 0, 3, 6, 9, 12, and 24 h post-gavage. General discomfort of treated mice was assessed
272 by observing them after gavage and throughout the experiment for signs of reduced mobility,
273 scruffy fur, hunched posture or changes in facial expression. Mice were sacrificed and
274 dissected after 24 h. Fecal samples and intestinal contents were immediately stored at -80°C
275 for metabolite analysis and 16S rRNA gene amplicon sequencing.
276

277 **Metabolite analysis**

278 For sulfide quantification, 20 µl subsamples were added to 300 µl 2 g/l zinc acetate solution
279 in the anaerobic tent. Fixed samples were quantified colorimetrically using the Infinite M
280 Nano+ microplate reader (Tecan, Austria), as described previously [38].
281 Capillary electrophoresis was used to quantify metabolites in the supernatants of human cell
282 cultures, in gut microcosms, in bacterial pure cultures, and in the fecal samples of germ-free
283 and conventional mice. Concentrations of SQ, SL, DHPS, lactate, and the short-chain fatty
284 acids (SCFAs) formate, succinate, acetate, propionate, butyrate, and valerate were quantified
285 using a 7100 capillary electrophoresis system (Agilent, United States). Mouse fecal samples
286 were prepared by adding 40 µl of ultrapure water to 0.01 g of feces. After mixing, samples
287 were centrifuged at 11,000 x g for 10 min at 4°C and supernatants were stored at -20°C. For
288 analysis, culture supernatants or metabolite extracts from fecal samples were diluted 1:5-
289 1:20 in ultrapure water containing 0.1 mM of an internal standard. Caproate, valerate or
290 succinate was used as an internal standard and was selected based on the sample
291 background. Analyte standard mixtures were prepared in concentrations of 0.025 mM, 0.05

292 mM, 0.1 mM, 0.25 mM, 0.5 mM and 1 mM. An organic acid buffer (Agilent, United States)
293 was used as a running buffer. The instrument's bare fused silica capillary (75 µm inner
294 diameter, 72 cm effective length; Agilent, United States) was flushed within the system for
295 four minutes as part of the preconditioning process before each measurement. Samples were
296 then injected at 50 mbar for five seconds. Measurements were performed at –25 kV, 100 µA,
297 and 6 W.
298 SQ and its degradation products DHPS, SL, isethionate, 3-HPS, 3-sulfopropionate, and
299 sulfoacetate in mouse gut content microcosms, *E. clostridioformis* pure cultures, and in fecal
300 samples of germfree and conventional mice were additionally quantified using liquid
301 chromatography-mass spectrometry. Samples were prepared by centrifuging at 18,000 x g for
302 5 minutes at 4°C. The supernatants were then diluted 1:10 with ultrapure water and mixed at
303 a 7:3 (v/v) ratio with ≥ 99.9% acetonitrile containing 6.7 mM para-toluenesulfonate as internal
304 standard. Samples were quantified using a LCMS-2020 single quadrupole mass spectrometer
305 system (Shimadzu, Japan) consisting of LC-40B XR pumps, a SIL-40C XR autosampler, a CTO-
306 40S column oven (heated to 30°C) and a MS-2020 electrospray ionization mass spectrometer.
307 Organosulfonate separation was carried out on an iHILIC-Fusion(+) column (100 × 2.1 mm, 3.5
308 µm, 100 Å), as described previously [39].
309

310 **16S rRNA gene amplicon sequencing and real-time PCR**

311 DNA extraction and 16S rRNA gene amplicon sequencing was performed by the Joint
312 Microbiome Facility of the Medical University of Vienna and the University of Vienna under
313 the project numbers JMF-2012-06 (human fecal microcosms), JMF-2108-01 (conventional
314 mouse experiment), JMF-2212-09 (mouse gut content microcosms). DNA was extracted with

315 the QIAamp Fast DNA Stool Mini Kit according to the manufacturer's protocol (Qiagen GmbH,
316 Austria). Extraction contamination was controlled for using blank extractions containing kit-
317 provided buffers alone. An established two-step PCR-barcoding method (H_515F_mod-5'-
318 (head) GCT ATG CGC GAG CTG C - GTG YCA GCM GCC GCG GTA A and H_806R_mod-5'-(head)
319 TAG CGC ACA CCT GGT A - GGA CTA CNV GGG TWT CTA AT) was used for 16S rRNA gene
320 amplicon sequencing of bacteria and archaea [40]. Prior to preparing the sequencing libraries,
321 barcoded amplicon libraries were normalized with the SequalPrep normalization plate kit and
322 subsequently pooled (TrueSeq Nano Kit; Illumina, United States) [40,41]. Amplicon
323 sequencing was performed on the MiSeq (V3, 600 cycles; Illumina, United States) and results
324 were analyzed according to the procedures outlined previously [40]. Amplicon sequence
325 variants (ASVs) were inferred using the DADA2 workflow [42] and taxonomically classified
326 with the SILVA database (release 138). Sequencing libraries were rarified and analyzed with
327 the software packages phyloseq (v1.42.0) [43] and vegan (v2.6-4) [44] for RStudio
328 (rstudio.com, R version 4.2.2). Principal coordinate analysis was performed using a Bray-Curtis
329 dissimilarity matrix computed with phyloseq. DESeq2 (v1.38.3) was used to perform
330 differential abundance analyses between treatment groups and time points [45].
331 In the human fecal microcosm experiment, ASV abundance at each time point and treatment
332 was compared to two controls: Its corresponding baseline at 0 h, and to the abundance in the
333 0.01 mM SQ incubation at the same time point. Notably, the 0.01 mM SQ incubation was used
334 as control because (i) metabolite data showed no significant differences compared to the
335 unamended control and (ii) only one control incubation was sequenced. The baseline at 0 h
336 served as control to identify ASVs with an increased abundance compared to the beginning
337 of the experiment. ASVs significantly enriched in both analyses were considered responsive
338 to the amendment. For the mouse gut content microcosm experiments, each treatment was

339 evaluated against the unamended control at each time point. In the conventional mouse
340 experiment, ASV abundance was compared to the baseline at 0 h for each treatment.
341 However, ASVs were considered significantly responsive to the amendment only, if they were
342 not also significantly enriched in the unamended control over time. Adjusted *p*-values of <0.01
343 were considered significant. The taxonomic classification of enriched ASVs in all experiments
344 was verified by Blastn against the NCBI 16S rRNA sequences database, excluding uncultured
345 and environmental sample sequences [46].
346
347 The total 16S rRNA gene copies were quantified by real-time PCR (CFX96 Real-Time System;
348 Bio-Rad Laboratories Ges.m.b.H, Austria). PCR reactions consisted of 10 µl iQ SyBr Green Mix
349 2x, 0.8 µl of each primer (0.4 µM), 6.4 µl sterile nuclease-free water, and 2 µl DNA extract.
350 The universal primers 515F (5'-GTG YCA GCM GCC GCG GTA A-3') [47] and 806R (5'-GGA CTA
351 CNV GGG TWT CTA AT-3') [48] targeting bacteria and archaea were used. The PCR program
352 started with an initial denaturation step at 95°C for 5 min followed by 40 cycles of 95°C for
353 30 s, 55°C for 30 s, and 72°C for 30 s. Final elongation was performed at 72°C for 2 min. A
354 negative control, i.e. water as template, was included in each run. Genomic DNA
355 of *Escherichia coli* K12 was used to prepare a standard serial dilution series of 10^9 (15.4 ng/µl
356 DNA of the standard) to 10^3 copy numbers of the 16S rRNA gene to generate a standard curve,
357 which was linear across the entire dilution series. The 16S rRNA gene copy numbers of
358 selected ASVs were calculated by multiplying their relative abundances with the total 16S
359 rRNA gene abundances determined by real-time PCR.
360

361 **Analysis of genomes from the mouse microbiome**

362 High-quality mouse microbiota-derived bacterial genomes were downloaded from the Mouse
363 Gastrointestinal Bacteria Catalogue (n=26640) [49]. Open reading frames were determined
364 using prodigal and subsequently annotated via HMSS2 [50]. Additional hidden Markov models
365 were generated for SQDG and DHPS conversion related proteins not represented in HMSS2,
366 as described previously [51]. Among others, this included isethionate reductase IsrBHDK [52],
367 DHPS-sulfolyase HpsGH, DHPS-dehydratase HpfGH [17], sulfopropionaldehyde reductase
368 HpfD, succinate semialdehyde dehydrogenase Ssadh [53], DHPS dehydrogenase DhpA, 3-
369 sulfolactaldehyde dehydrogenase SlaB [16] and sulfoquinovosidase SqgA [7] (Table S1). For
370 all hidden Markov models, a general bitscore cutoff of 100 was chosen to detect homologs.
371 All hits were tested for co-location in the respective genome with a maximum distance of
372 3500 nucleotides between genes, as described before [51]. The resulting gene clusters were
373 then searched for patterns of genes with the same sequential occurrence using a custom
374 implementation of the colinear syntenic blocks finder algorithm [54], with a tolerance of two
375 gene insertions and a length of four co-located genes. This was done to ensure enzyme
376 function in the respective metabolism by sequence similarity and genetic vicinity.

377

378 **Results**

379 **SQ is not degraded by human HT-29 cells *in vitro***

380 To test whether SQ is degraded by human intestinal cells, we incubated HT-29 human
381 colorectal cancer cells with and without SQ. SQ concentrations in cell culture supernatants
382 from both SQ-supplemented DMEM and glucose-free DMEM remained unchanged

383 throughout the experiment (Figure 2 a, b). Lactate was only produced in glucose-containing
384 incubations (Figure 2 c, d). The effect of increasing glucose or SQ concentrations on HT-29 cell
385 growth in DMEM was similar for both substrates. Protein production was fully inhibited only
386 in cultures treated with very high, non-physiological concentrations (250 mM) of glucose or
387 SQ (Figure 2 e, f). Overall, these findings suggested that SQ is not degraded and metabolized
388 by human cells *in vitro*. A potential limitation of using cancer cells is that their metabolism
389 does not necessarily reflect the metabolism of primary cells [55].
390

391 **^{13}C-labeled SQ is not respired to ^{13}C-CO_2 by germ-free mice**

392 Next, we employed stable isotope tracing with ^{13}C-SQ in germ-free mice to study potential SQ
393 degradation by mammalian cells *in vivo*. Germ-free mice received a single dose (10 mg) of
394 either fully labeled ^{13}C-SQ or ^{13}C-glucose and their respired air and fecal samples were
395 subsequently collected over a 24-hour period for $^{13}CO_2$ breath tests and metabolite analysis,
396 respectively. Mice administered ^{13}C-SQ did not produce $^{13}CO_2$. Contrarily, mice receiving ^{13}C-
397 glucose produced up to 117 µg $^{13}CO_2$/min at one hour post-gavage (Figure 2 g). In mice
398 gavaged with ^{13}C-SQ, SQ was detected in fecal samples already one hour after its
399 administration (Figure 2 h). Yet, SQ degradation metabolites were not detected in the feces.
400

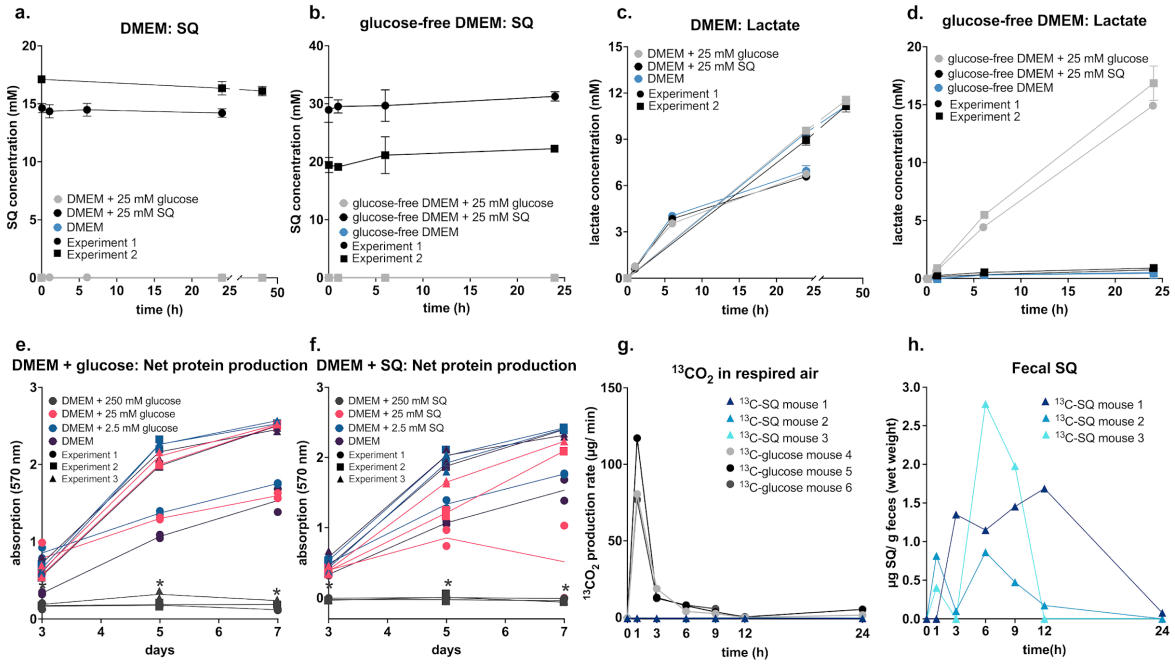

Figure 2: SQ was not metabolized by human intestinal cells and germ-free mice. SQ was not degraded by HT-29 cells in DMEM medium amended with 25 mM SQ (shown in black) (a). SQ was not degraded by HT-29 cells in glucose-free DMEM medium amended with 25 mM SQ (shown in black) (b). HT-29 cells produced lactate independent of the treatment in DMEM medium (c). In glucose-free DMEM, HT-29 cells produced lactate only in incubations amended with 25 mM glucose (shown in grey) (d). Protein production was inhibited in incubations with 250 mM glucose (shown in dark grey), but not in incubations with 25 mM glucose (shown in pink) and 2.5 mM glucose (shown in blue) (e). Protein production was inhibited in incubations with 250 mM SQ (shown in dark grey), but not in incubations with 25 mM SQ (shown in pink) and 2.5 mM SQ (shown in blue) (f). Each germ-free mouse (n = 3 per group) was gavaged with 10 mg of fully labeled ^{13}C-glucose or ^{13}C-SQ. (g). Glucose, but not SQ, was respired by germ-free mice as shown by $^{13}CO_2$ production via breath air isotope analysis. SQ was repeatedly detected in the feces of all mice gavaged with ^{13}C-SQ within 24 h after the gavage (h). In a., b., c., and d., lines show averages of triplicate incubations with error bars representing one standard deviation. Two experiments were conducted varying only slightly in the sampling time points. Different data point shapes indicate the two experiments. In e. and f., lines show averages of duplicate measurements and data points show individual values. Different data point shapes represent the three conducted experiments. Asterisks mark significant differences between a treatment group and the control (DMEM medium without amendment) at each time point. Significant differences were determined by ANOVA with Dunnett's post hoc test. Adjusted *p*-values smaller than 0.05 were regarded as significant. SQ, sulfoquinovose; DMEM, Dulbecco's Modified Eagle Medium.

Response of the microbiota to different doses of SQ in human fecal microcosms

We performed anoxic incubations with human fecal microcosms to assess the dose-dependent effects of SQ (0.01 mM, 0.1 mM, 1 mM, and 10 mM) on metabolite production and gut microbiota composition (Figure 3 a). Only the microcosms with high SQ concentrations (1 mM, 10 mM) consistently showed significant differences in metabolite levels compared to the unamended control (Figure S1). The temporal dynamics of SQ

427 degradation and the production of metabolic products were consistent between the 1 mM
428 and 10 mM SQ treatments (Figure 3 b, c). SQ was mostly degraded within 12 h, coinciding
429 with the production of DHPS. In comparison, SL and sulfide were produced later and
430 represented only a smaller fraction of the produced sulfur metabolites within the 24 h
431 incubation. SQ, DHPS, and SL were not detected in the unamended control incubation (Figure
432 3 d). The production of acetate and butyrate, known SQ degradation products [15,16,39],
433 increased significantly in the 1 mM and 10 mM SQ treatments compared to the unamended
434 control (Figure 3 e, f).
435 Changes in total microbial abundance during the 24 h incubation period were quantified by
436 16S rRNA gene-targeted real-time PCR (Figure 3 g). Gene copy numbers decreased in
437 microcosms without SQ and with 0.01 or 0.1 mM SQ and remained transiently constant in
438 microcosms with 1 mM SQ. A significant increase in gene copy numbers was only observed in
439 microcosms with 10 mM SQ.
440 We performed 16S rRNA gene amplicon sequencing and differential abundance analyses to
441 identify amplicon sequence variants (ASVs) with increased relative abundance in SQ-amended
442 incubations and thus a possible role in SQ degradation. Significantly enriched ASVs were only
443 detected in incubations with concentrations of 0.1 mM SQ or higher; one, two, and fourteen
444 ASVs were enriched in microcosms with 0.1, 1, and 10 mM SQ, respectively (Table S2, Figure
445 S2). *Escherichia/Shigella* ASV 8 was enriched at all three SQ concentrations, *Waltera*
446 *intestinalis* ASV 7 was enriched at 1 and 10 mM SQ, while the following ASVs were only
447 enriched at 10 mM SQ: *A. rectalis* ASV 1, *Alistipes shahii* ASV 2, *Ruminococcus bromii* ASV 3,
448 *Oscillospiraceae* ASV 5, *B. wadsworthia* ASV 6, *Enterocloster citroniae* ASV 9, *Phocaeicola*
449 *dorei* ASV 4, *Phocaeicola massiliensis* ASV 12, *Phocaeicola vulgatus* ASV 14, *Bacteroides*
450 *xylanisolvens* ASV 10, *Bacteroides caccae* ASV 11, and *Bacteroides ovatus* ASV 13. Variations

451 in the dose-response patterns of SQ-responsive microorganisms are not yet fully explained
452 but may result from differences in SQ metabolic energetics and enzyme kinetics. Close
453 relatives of some of the enriched ASVs (Figure 3 h, i, j) have been physiologically confirmed to
454 degrade SQ (*A. rectalis*, *E. coli*) or DHPS (*B. wadsworthia*) [10,15]. Furthermore, members of
455 the genera *Enterocloster* and *Ruminococcus* encode the sulfofructose-transaldolase pathway
456 [15]. Together with a member of *Alistipes*, members of these genera/species have also
457 previously been significantly enriched in human fecal microcosms amended with 10 mM SQ
458 [15]. ASVs related to these taxa generally showed a continuous increase in absolute
459 abundance over the 24 h incubation, which coincided with the kinetics of SQ disappearance
460 and DHPS production (Figures 3 and S2). In contrast, ASVs of *Phocaeicola* and *Bacteroides*
461 showed an initial spike in absolute abundances at 6 h followed by a decline, suggesting they
462 are not directly involved in SQ degradation (Table S2, Figure S2). Type strain genomes of the
463 most closely related *Alistipes*, *Waltera*, *Bacteroides* or *Phocaeicola* species do not encode
464 known SQ or DHPS degradation pathways.

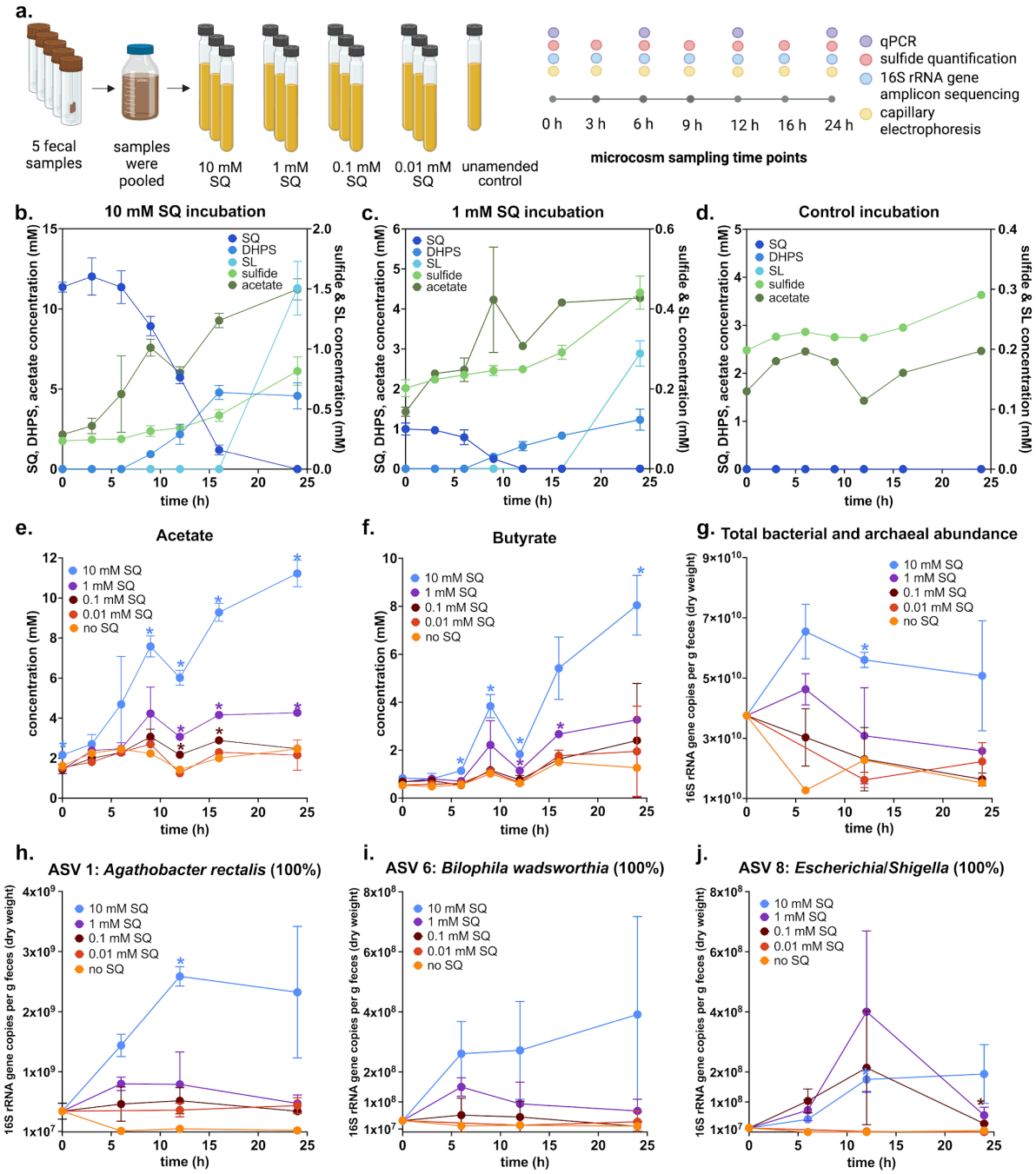

Figure 3: Metabolite dynamics and differential responses of microbiota members to different doses of SQ in 24 h human fecal microcosm incubations. Overview of the experimental and analytical approach (created with biorender.com) (a). Sulfur metabolite dynamics in incubations amended with 10 mM SQ (b), 1 mM SQ (c), and in the unamended control (d). SQ, DHPS, and SL were not detected in unamended control microcosms. Higher doses of SQ led to increased concentrations of acetate (e) and butyrate (f). No significant differences in acetate concentrations were detected between incubations with 0.01 mM SQ (shown in red) and unamended controls (shown in orange). No significant differences in butyrate concentrations were detected between incubations with 0.1 mM SQ (shown in dark red) or 0.01 mM SQ (shown in red) and unamended controls (shown in orange). Changes in absolute bacterial and archaeal 16S rRNA gene copy numbers in the microcosm incubations with different SQ doses (g). Changes in the absolute abundance of *A. rectalis* ASV 1 (h), *B. wadsworthia* ASV 6 (i), and *Escherichia/Shigella* ASV 8 (j). The 16S rRNA gene sequence similarity (%) to the closest, named relative is shown for each ASV. In b., c., e., f., g., h., i., and j., the lines show the average of triplicate incubations with error bars representing one standard deviation. Only a single incubation was performed for the unamended control microcosm. Coloured asterisks show significant differences between the respective treatment (n = 3) and the retrospectively designated control incubations (n = 4, consisting of three 0.01 mM SQ incubations and one unamended control) at individual time points. Significant differences

480 were determined by ANOVA with Dunnett's post hoc test. Adjusted *p*-values smaller than 0.05 were regarded as significant.
481 SQ, sulfoquinovose; DHPS, 2,3-dihydroxypropane-1-sulfonate; SL, 3-sulfolactate; ASV, amplicon sequencing variant.

482

483 **Incomplete SQ degradation in mouse gut content microcosms**

484 Two independent microcosm experiments were performed with pooled gut contents of mice
485 and amended with SQ or DHPS to investigate the SQ metabolism (Figure 4 a). In experiment
486 1, microcosms containing entire gut contents were incubated with either 10 mM SQ or 10
487 mM DHPS. Following a lag phase of over 24 hours, SQ degradation to DHPS was observed in
488 SQ-amended incubations at a near 1:1 ratio, as measured by liquid chromatography-mass
489 spectrometry (Figure 4 b). SL, sulfoacetate, and 3-HPS were not detected. Yet, small amounts
490 of isethionate (0.01 mM after 48 h and 0.02 mM after 96 h) were detected (Figure S3). Sulfide
491 concentrations in SQ-amended microcosms increased slightly, remaining below 1 mM, and
492 did not correlate with SQ degradation in timing or stoichiometry. Capillary electrophoresis
493 analysis of SCFAs showed an increase in acetate production in SQ-amended incubations, from
494 5 mM to 11.1 mM over 96 h, compared to the control incubation, from 2.6 mM to 4.3 mM
495 (Figure 4 b). Concentrations of DHPS and acetate remained constant in DHPS-amended
496 incubations (Figure 4 c). Sulfide concentrations were significantly higher in DHPS-amended
497 incubations compared to SQ-amended incubations and unamended controls. However, the
498 small increase from 0.2 mM to 0.5-0.6 mM sulfide in the DHPS-amended incubations
499 compared to 0.3-0.4 mM sulfide in the unamended control did not suggest a quantitative
500 turnover of DHPS to sulfide (Figure 4 c). SQ and DHPS were not detected in the unamended
501 control incubations, and sulfide concentrations remained below 0.4 mM (Figure 4 d).
502 Microbial abundances decreased over time in all microcosms, but remained significantly
503 higher in SQ incubations from 48 h onwards (Figure S4). Microbial abundances decreased
504 from 1.8 ± 0.7 x 10^{10} 16S rRNA gene copies/g dry weight to 5.2 ± 1.0 x 10^{9} 16S rRNA gene

505 copies/g dry weight in SQ-amended microcosms and to 5.3 ± 1.4 x 10^8 16S rRNA gene copies/g
506 dry weight in the unamended controls.
507 Differential abundance analysis of 16S rRNA gene amplicon sequencing data identified nine
508 ASVs enriched in the 10 mM SQ incubations compared to unamended controls (Figure S5).
509 *Escherichia/Shigella* ASV 8 had the highest $\log_2$ fold change of all enriched ASVs and its
510 absolute abundance dynamic corresponded to the turnover of SQ into DHPS (Figure 4 b, e).
511 Other enriched ASVs included *Lachnospiraceae* ASV 15, *Bacteroides acidifaciens* ASV 16,
512 *Bacteroides* ASV 19, *F. rodentium* ASV 17, *Coprobacillaceae* ASV 18, *Ruminococcus* ASV 20,
513 *Prevotellaceae* ASV 21, and *P. vulgatus* ASV 14 (Table S3). Notably, *Escherichia/Shigella* ASV 8
514 and *P. vulgatus* ASV 14 were enriched in both human fecal microcosms and mouse gut
515 content microcosms with SQ. In contrast to SQ-amended incubations, temporal changes in
516 microbial community composition in the DHPS-amended incubations were indistinguishable
517 from control incubations and no ASVs were identified as enriched (Figure 4 f).
518
519 For experiment 2, separate microcosms for small intestinal contents and cecal contents were
520 each incubated with 10 mM SQ and analyzed for changes in microbial community composition
521 compared to unamended control incubations. Microbial 16S rRNA gene copy numbers
522 decreased in control incubations, while remaining rather constant in cecal incubations with
523 SQ or decreased less in small intestinal incubations with SQ compared to the control (Figure
524 S4). Seven ASVs were significantly enriched in small intestinal incubations and four ASVs in
525 cecal incubations. ASVs in small intestinal incubations were *Enterococcus* ASV 22 and 23,
526 *Enterocloster* ASV 24, 25, and 26, *Ligilactobacillus* ASV 27, and *Akkermansia muciniphila* ASV
527 28 (Figure 4 g, Table S3). In cecal incubations, enriched ASVs belonged to *Escherichia/Shigella*
528 ASV 8, *Parabacteroides distasonis* ASV 29 and 30 and, *Enterocloster* ASV 25 (Figure 4 h, i, Table

529 S3). In contrast to the other ASVs, the absolute abundances of *Ligilactobacillus* ASV 27 and *A.*

530 *muciniphila* ASV 28 decreased during the incubation and thus are unlikely to be involved in

531 primary SQ degradation (Figure S6).

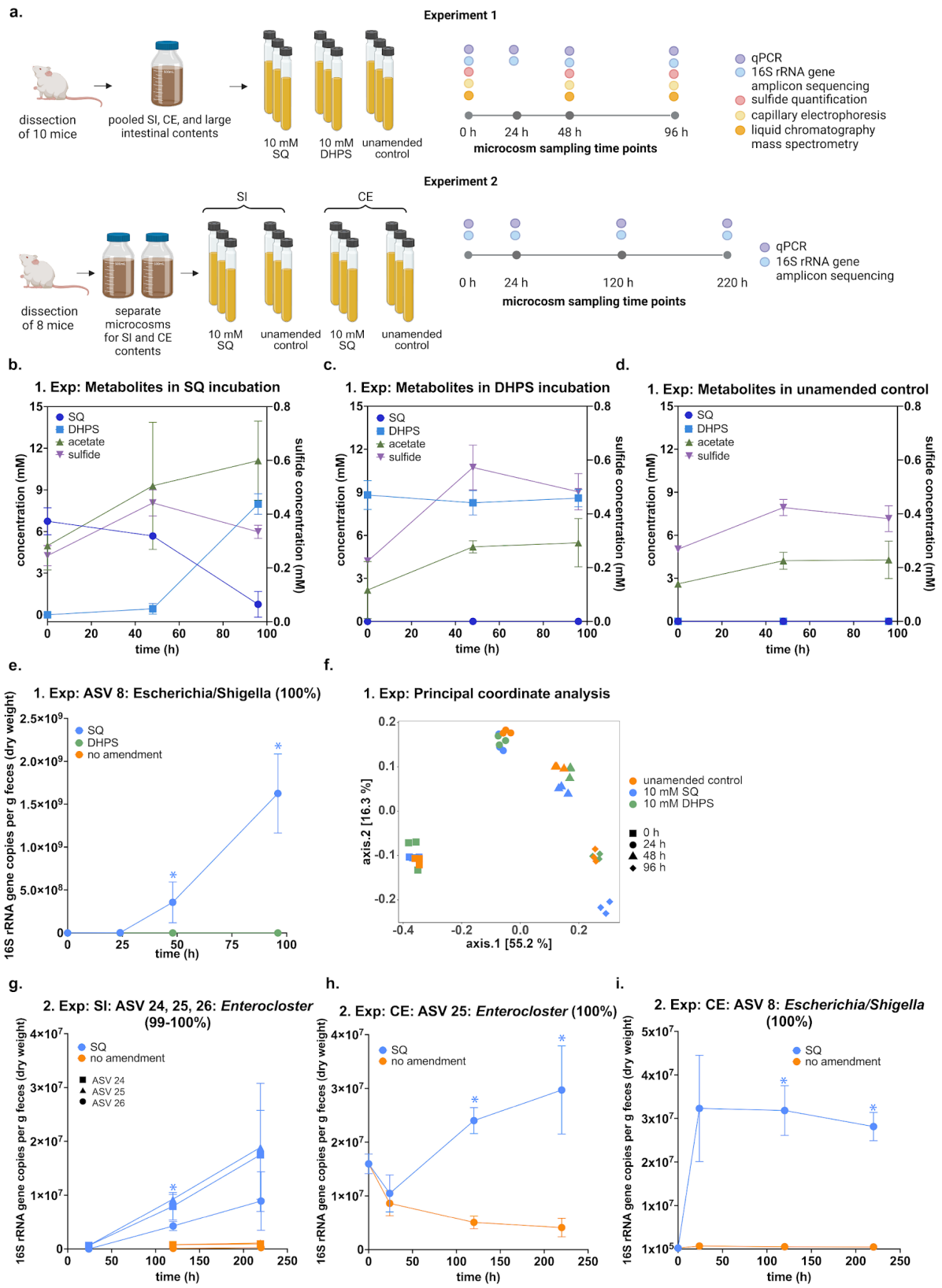

Figure 4: Metabolite dynamics and differential responses of microbiota showed that SQ, but not DHPS, was degraded in murine gut content microcosms. Overview of the experimental and analytical approach (created with biorender.com) (a). Metabolite dynamics in gut content microcosms (Experiment 1: pooled small intestinal, cecal, and large intestinal contents) incubated with 10 mM SQ (b), 10 mM DHPS (c), and without amendment (control) (d). SQ and DHPS were not detected in control incubations. Calculated absolute 16S rRNA gene abundance of *Escherichia/Shigella* ASV 8 in incubations of experiment 1 (e). Principal coordinate analysis plot of beta diversity (Bray-Curtis dissimilarity) of 16S rRNA gene amplicon

539 data from incubations of experiment 1 (f). Calculated absolute 16S rRNA gene abundance of selected ASVs that were
540 significantly enriched in SQ-amended mouse small intestinal content and cecum content incubations of experiment 2 (g-i).
541 The 16S rRNA gene sequence similarity (%) to the closest, named relative is shown for each ASV. The lines in b., c., d., e., g.,
542 h. and i. show averages of triplicate incubations with error bars representing one standard deviation. Coloured asterisks
543 show significant differences between the respective treatment and the unamended control at individual time points.
544 Significant differences were either determined by two-way ANOVA with Dunnett post hoc test (1. experiment: pooled gut
545 content) or by multiple unpaired t-tests with Holm-Šidák post hoc test (2. experiment: small intestine and cecum). Adjusted
546 *p*-values smaller than 0.05 were regarded as significant. SQ, sulfoquinovose; DHPS, 2,3-dihydroxypropane-1-sulfonate; Exp,
547 experiment; SI, small intestine; CE, cecum; ASV, amplicon sequencing variant.

548

549 **SQ is degraded to DHPS in conventional wild type mice**

550 To investigate SQ metabolism by the mouse gut microbiota *in vivo*, we gavaged a single dose
551 of either 1 mg SQ or 10 mg SQ to conventional wild type laboratory mice and collected fecal
552 samples up to 24 h post-gavage (Figure 5 a). Mice fed with SQ showed no signs of digestive
553 problems or general discomfort. While the water content of fecal pellets was not measured,
554 the consistency of fecal pellets remained stable throughout the experiment, with no visible
555 difference between the tap water control and SQ-treated mice. Fecal metabolites were
556 analyzed via capillary electrophoresis as well as liquid chromatography-mass spectrometry
557 (Table S4). SQ was detected in mice receiving 10 mg SQ between 3 and 6 h post-gavage, while
558 DHPS appeared at 6 h and remained detectable in some mice until the end of the experiment
559 (Figure 5 b, Figure S7). Additionally, taurine as well as small amounts of 3-sulfolactate,
560 sulfoacetate, and isethionate were measured via liquid chromatography-mass spectrometry
561 in mice receiving 10 mg SQ (Table S4). Taurine and isethionate were detected already at the
562 beginning of the experiment, indicating that the presence of these metabolites was
563 independent from SQ addition. Temporal dynamics of SCFA concentrations, total 16S rRNA
564 gene copy numbers, and microbial composition were not significantly different between the
565 three treatment groups (Figure 5 c - g).

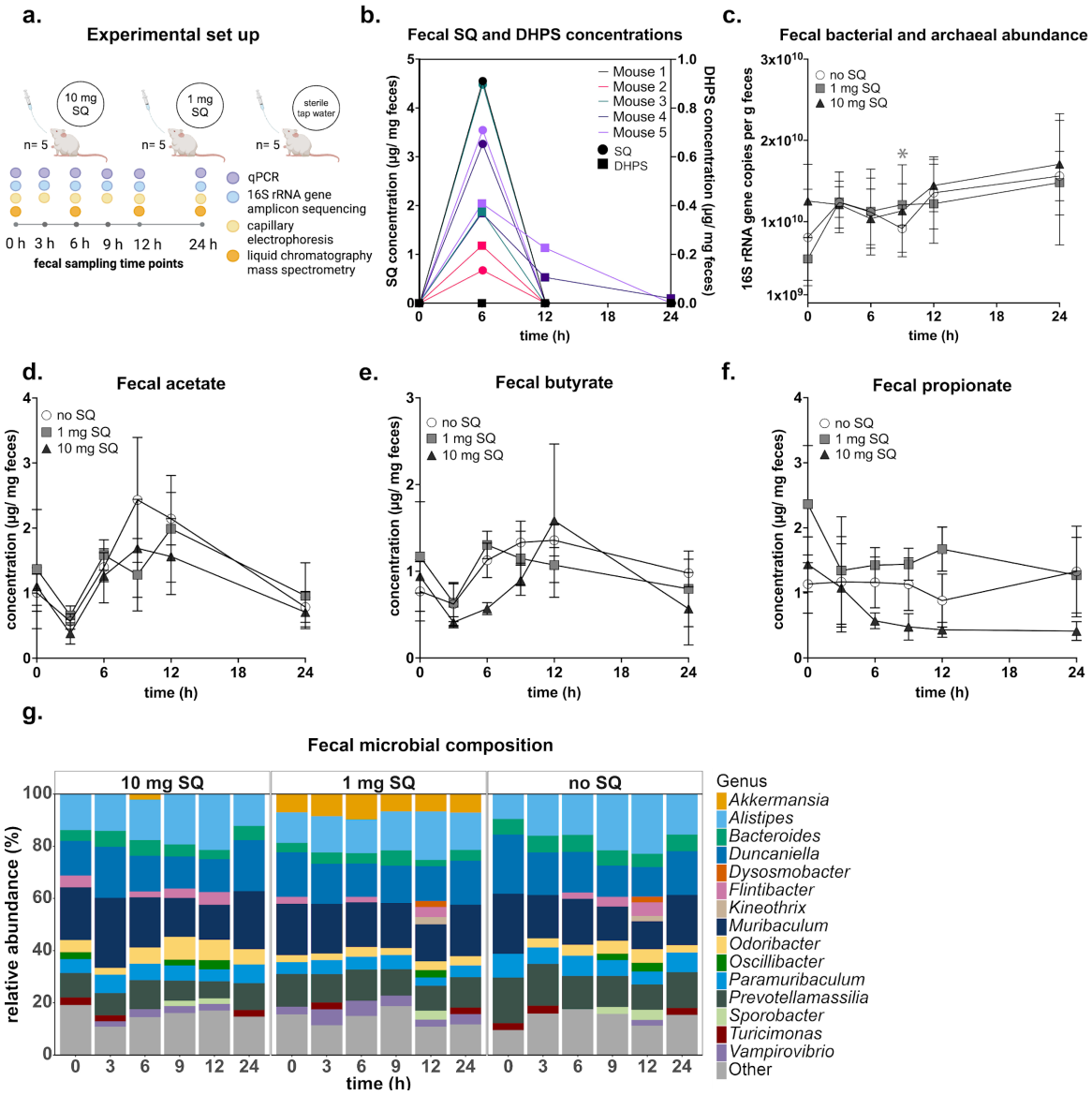

Figure 5: Fecal metabolite and microbial community dynamics of conventional wild type mice over 24 h after receiving a single dose of SQ. Overview of the experimental and analytical approach (created with biorender.com) (a). Concentrations of SQ (circles) and DHPS (boxes), as analyzed by liquid chromatography-mass spectrometry, in feces of mice (n = 5) that each received a single dose of 10 mg SQ by gavage (b). Metabolite concentrations of all treatment groups, as analyzed by capillary electrophoresis, are depicted in Supplementary Table S4 and Figure S7. Total bacterial and archaeal 16S rRNA gene copy numbers in feces of the three treatment groups (c). Five biological replicates were measured in triplicate qPCR assays. The line shows the mean and the error bars represent one standard deviation. Concentrations of acetate (d), butyrate (e), and propionate (f) in feces of the three treatment groups. Mean values of five biological replicates are shown and error bars depict one standard deviation. Mean relative 16S rRNA gene abundance of dominant bacterial genera in feces of the three treatment groups (g). All genera below an abundance of 2% are summarized in 'Other'. All data refer to the wet weight of the feces. Asterisks show significant differences between the respective treatment and the tap water control at individual time points. Significant differences in c., d., e., and f. were determined by ANOVA with Dunnett's post hoc test. Adjusted *p*-values smaller than 0.05 were regarded as significant. SQ sulfoquinovose, DHPS 2,3-dihydroxypropane-1-sulfonate.

581 **SQDG/SQ and DHPS degradation pathways are encoded in few bacterial**
582 **genomes from the mouse gut**

583 We comprehensively examined the genetic potential for SQDG/SQ and DHPS degradation in
584 the mouse microbiota by analyzing the collection of 26640 metagenome-assembled genomes
585 (MAGs) from the Mouse Gastrointestinal Bacteria Catalogue for presence of the respective
586 pathways [49]. Our analysis revealed SQDG/SQ and DHPS degradation pathways in only 0.3%
587 (n=76) and 0.2 % (n=48) of all MAGs and in 16 (1.5%) and 8 (0.7%) of the 1094 species-level
588 genome bins, respectively (Figure 6 a, b). The sulfofructose-transaldolase pathway was
589 encoded in 57 MAGs, primarily from *E. clostridioformis*, *Otoolea symbiosa* (formerly
590 *Clostridium symbiosum*), and *E. aldenensis*, and represented the most prevalent SQDG/SQ
591 degradation pathway in the mouse microbiome (Figure 6 a). The sulfo-Embden-Meyerhof-
592 Parnas pathway was encoded in 13 *Enterobacteriaceae* MAGs. The sulfo-transketolase
593 pathway was encoded in 6 *Oscillibacter* MAGs. Key enzymes in DHPS degradation pathways
594 (Figure 1 b) were encoded in 48 MAGs across five genera. These included 16 MAGs with *hpsN*,
595 12 MAGs with *dhpA*, 10 MAGs with *hpfGH*, 8 MAGs with *hpsGH*, and 2 MAGs with both *hpsGH*
596 and *dhpA* (Figure 6 b). These pathways could generate sulfite intracellularly and were present
597 in the sulfidogenic genera *Desulfovibrio*, *Taurinivorans*, *Mailhella*, and *Bilophila* that employ
598 a DsrAB-dissimilatory sulfite reductase to respire sulfite to H_2S [15,16,19]. Nine *E.*
599 *clostridioformis* MAGs and one *E. aldenensis* MAG encoded the fermentative *hpfGHD*
600 pathway along with the sulfofructose-transaldolase pathway, suggesting these bacteria may
601 ferment SQ via DHPS also to 3-HPS [17].

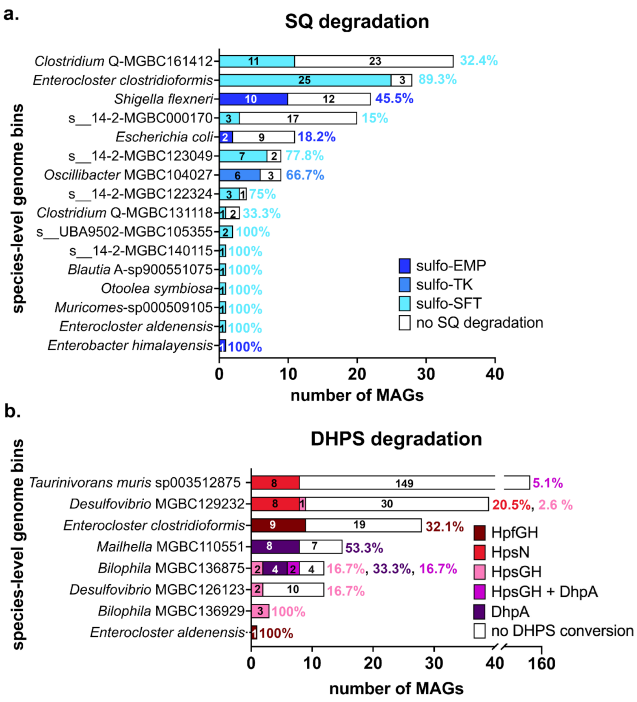

Figure 6: Analysis of microbial genomes revealed genetic SQDG/SQ and DHPS degradation potential is sparsely distributed in the mouse microbiome. Distribution of SQDG/SQ (a) and DHPS (b) degradation potential across a collection of 26,640 microbial MAGs from the mouse intestinal tract. Species-level genome bins are ordered based on the total number of genomes. The total and relative (%) number of genomes that encode a specific SQDG/SQ or DHPS pathway (shown in different colors) is indicated for each species-level genome bin. Sixteen (represented by 76 MAGs) and eight (represented by 48 MAGs) species-level genome bins, contained complete gene clusters for SQDG/SQ and DHPS degradation, respectively. Some MAGs of *E. clostridioformis* and *E. aldenensis* encoded both SQDG/SQ and DHPS degradation pathways. MAG, metagenome-assembled genome; sulfo-EMP, sulfoglycolytic Embden-Meyerhof-Parnas pathway; sulfo-ED, sulfoglycolytic Entner–Doudoroff pathway; sulfo-SFT, sulfoglycolytic sulfofructose-transaldolase pathway; SQ, sulfoquinovose; DHPS, 2,3-dihydroxypropane-1-sulfonate; HpsG, DHPS-sulfolyase; HpsH, DHPS-sulfolyase activating enzyme; HpfG, DHPS-dehydratase; HpfH, DHPS-dehydratase activating enzyme; HpsN, DHPS-1-dehydrogenase; DhpA, dehydrogenase.

Enterocloster clostridioformis degrades SQ to DHPS in pure culture

Our mouse gut content microcosm experiments and genome analyses revealed members of the genus *Enterocloster* as SQ degraders. We thus performed anaerobic growth tests with the mouse strain *E. clostridioformis* YL32, which shares 100%, 99.6%, and 99.2% 16S rRNA gene sequence identity with the enriched ASVs 25, 24, and 26 in the mouse gut microcosms, respectively. Initial growth of strain YL32 in diluted or undiluted rich medium did not differ, regardless of SQ supplementation. However, cultures supplemented with SQ exhibited a secondary growth phase during the late stationary phase, achieving significantly higher optical densities than cultures without SQ. This secondary growth was more pronounced in

624 diluted rich medium (Figure 7 a). Diauxic growth in SQ-supplemented cultures indicated that
625 SQ supported growth only after energetically more favorable substrates in the rich medium
626 were consumed. This was supported by the timing of SQ degradation, which concurred with
627 the second growth phase after 100 h. SQ was degraded nearly stoichiometrically to DHPS
628 (Figure 7 b) while sulfide production did not differ significantly between cultures with and
629 without SQ (Figure 7 c). Although *E. clostridioformis* YL32 possesses the genetic potential to
630 ferment DHPS further (Figure 7 d), the DHPS fermentation product, 3-HPS, was not detected.

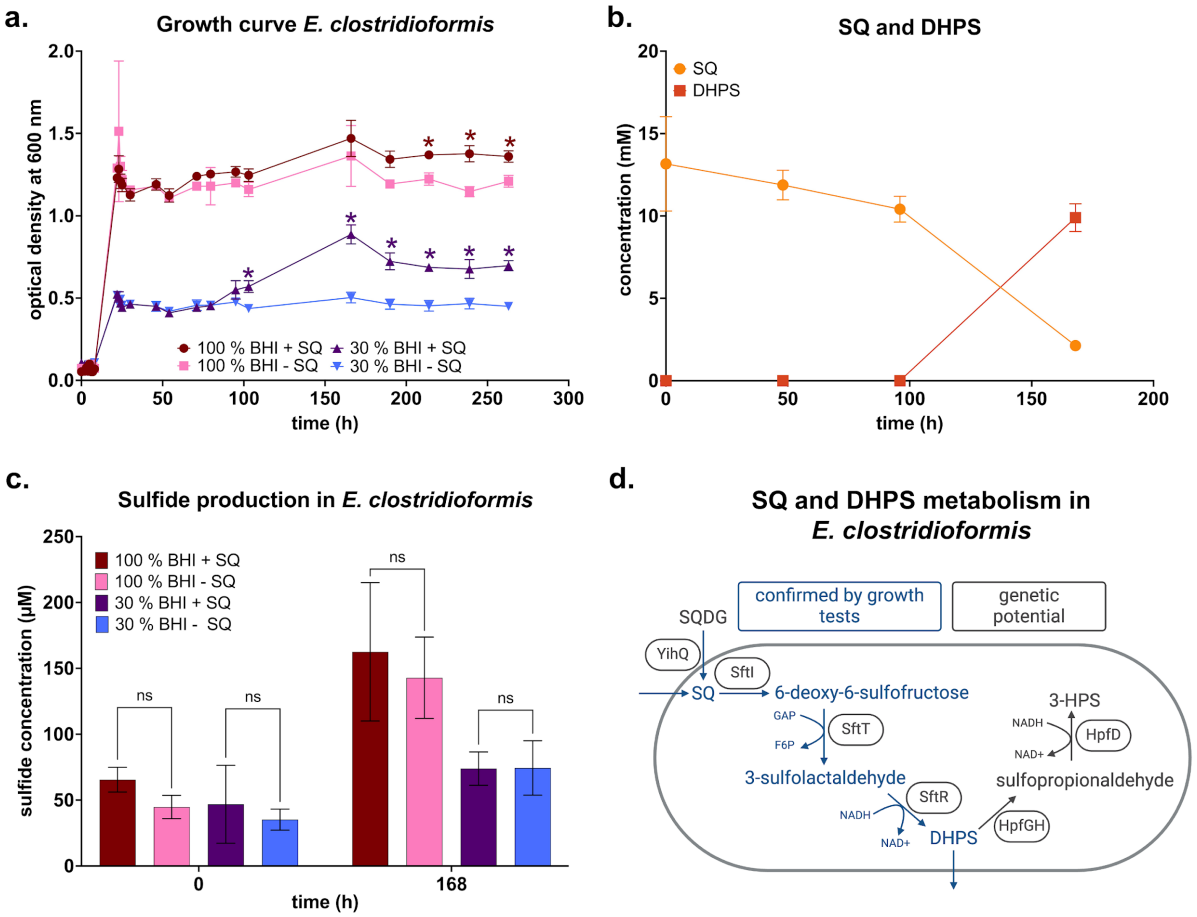

631

632 **Figure 7: A pure culture of *Enterocloster clostridioformis* anaerobically degraded SQ to DHPS.** Anaerobic growth tests of *E.*
633 *clostridioformis* strain YL32 with 10 mM SQ (a). SQ triggered a second growth phase of *E. clostridioformis* in diluted (30%)
634 rich medium (a) that coincided with a decrease of SQ and an increase of DHPS at a stoichiometry of about 1:1 (b). Small
635 amounts of sulfide were produced in all treatments but there were no significant differences between the sulfide produced
636 in incubations amended with SQ compared to unamended control incubations (c). Schematic overview of the proposed SQ
637 and DHPS pathways of *E. clostridioformis* YL32 (genome assembly number GCA_016696785) based on the growth tests and
638 genome analysis (created with biorender.com) (d). SQ can either be imported via the transporter SftA or cleaved from SQDG
639 by the sulfoquinovosidase YihQ (gene locus tag I5Q83_09300). SQ is converted to 6-deoxy-6-sulfofructose via the SQ
640 isomerase SftI (gene locus tag I5Q83_09270). The 6-deoxy-6-sulfofructose transaldolase SftT (gene locus tag I5Q83_09315)
641 catalyzes the transfer of a C3-moiety from 6-deoxy-6-sulfofructose to glyceraldehyde-3-phosphate (GAP), forming fructose
642 6-phosphate (F6P). The resulting 3-sulfolactaldehyde is then reduced to DHPS by the 3-sulfolactaldehyde reductase SftR
643 (gene locus tag I5Q83_09310). The DHPS dehydratase HpfG (gene locus tag I5Q83_10645) and its activating enzyme HpfH

(gene locus tag I5Q83_10640) catalyze the cleavage of the CO-bond of DHPS to form sulfopropionaldehyde, which is then reduced by the sulfopropionaldehyde reductase HpfD (gene locus tag I5Q83_10625) to 3-HPS. In a., b., c., lines/bars show averages of triplicate incubations with error bars representing one standard deviation. In a., coloured asterisks show significant differences between treatment groups and their respective control groups without SQ. In c., brackets show non-significant results in pairwise comparisons of treatment groups and their respective unamended control. Significance was tested using ANOVA with Tukey's post hoc test. Adjusted *p*-values smaller than 0.05 were regarded as significant. SQ, sulfoquinovose; BHI, brain-heart infusion medium; DHPS, 2,3-dihydroxypropane-1-sulfonate; 3-HPS, 3-hydroxypropane-1-sulfonate; ns, not significant; SQDG, sulfoquinovosyldiacylglycerol.

Additionally, we tested SQ degradation by the mouse strain *F. rodentium* ALO17, which shares 100% identity with an ASV enriched in the mouse gut microcosms. However, growth of strain ALO17 was not significantly different between cultures with and without SQ. Also, SQ degradation and formation of degradation products were not detected (Figure S8). These results are in line with the absence of known SQ and DHPS pathway genes in the *F. rodentium* ALO17 genome.

Discussion

SQ in the gut exclusively derives from dietary intake, primarily of green edible plants (e.g. spinach, green onions) and edible micro- and macroalgae (e.g. spirulina, nori) that contain the ubiquitous thylakoid membrane lipid SQDG. In the mammalian gut, pancreatic lipases hydrolyze SQDG to sulfoquinovosyl glycerol [56,57]. Subsequently, SQ is cleaved off from SQDG or sulfoquinovosyl glycerol by sulfoquinovosidases [6,7], key enzymes of certain gut bacteria that take up SQ for further respiration or fermentation. SQ is structurally analogous to glucose-6-phosphate and was initially proposed to be degraded via a pathway similar to glycolysis [58,59]. Since the first discovery of sulfoglycolysis in bacteria [10], further sulfoglycolytic pathways have been described in different bacterial taxa [8,9,11–14]. While plants [58] and algae [60] can also degrade SQ via yet unknown pathways, it was unclear if animals are capable of SQ degradation and if mammalian cells are involved in intestinal SQ

672 metabolism. Here, we show that SQ is neither metabolized by human colorectal
673 adenocarcinoma (HT-29) cells *in vitro* nor respired to CO_2 by germ-free mice *in vivo*. This
674 suggests that SQ cannot be metabolized by mammals, and instead serves exclusively as a
675 nutrient and growth substrate for specialized bacteria in the animal gut.
676
677 *A. rectalis* was previously shown to be the most dominant SQ-degrading species in human
678 fecal samples. Other species, including *F. prausnitzii*, *E. aldenensis* (formerly *Clostridium*
679 *aldenense*), *E. clostridioformis* (formerly *Clostridium clostridioforme*), and *Roseburia* sp.
680 AM16-25 also contributed to transcription of sulfofructose-transaldolase pathway genes in
681 the fecal microbiome [15]. Transcription of the sulfo-Embden-Meyerhof-Parnas pathway of
682 *Enterobacteriaceae* such as *E. coli* was considerably less important. Additionally, *B.*
683 *wadsworthia* was identified as the dominant degrader of DHPS, which is produced by the
684 primary SQ fermenters [15]. Our human fecal microcosm experiments with different SQ doses
685 corroborated the relevance of *A. rectalis* and *B. wadsworthia* for complete SQ degradation to
686 H_2S in the human gut. We further revealed that a minimum concentration of 0.1 mM SQ was
687 sufficient to induce significant changes in the absolute abundance of selected microbiota
688 members. The total amount of SQ in 10 ml microcosms amended with 0.1 mM SQ
689 corresponds to the SQ content in about 11 g of fresh spinach (Table S5), the edible plant with
690 the highest known SQDG concentration [3,61]. These results align with previous findings
691 showing that SQ degradation ranks among the top third of all transcribed metabolic pathways
692 of the fecal microbiome, establishing it as a microbial core function in the human gut [15].
693 Intestinal SQ levels reached by regular dietary intake of green vegetables may thus impact gut
694 microbiota composition and potentially affect human health via SQ degradation metabolites
695 [15]. The main SQ fermentation products are formate, acetate, and DHPS [10,13,16,62].

696 Besides acetate formation, our human fecal microcosm experiments also revealed a
697 significantly higher butyrate concentration in microcosms amended with 10 mM SQ
698 compared to the control (Figure 3 f). Increased butyrate production during SQ degradation
699 has not been observed in previous SQ-amended human fecal microcosms [15], which suggests
700 it may be specific to the mixture of human fecal samples used in our study. While the reason
701 for the increased butyrate production remains unknown, it is likely produced by *A. rectalis*
702 and other bacteria that were enriched in the SQ-amended microcosms. *A. rectalis* and
703 relatives of other enriched ASVs (e.g. *W. intestinalis*) can produce butyrate from fermentation
704 of carbohydrates [63–65]. Butyrate production by *A. rectalis* involves the acetyl-CoA pathway,
705 with butyryl-CoA:acetate CoA-transferase (But) as the key terminal enzyme that generates
706 butyrate from two acetyl-CoA molecules and acetate as co-substrate [66–69]. *Faecalicatena*
707 sp. DSM22707, an isolate from petroleum reservoir produced water, produces butyrate and
708 other metabolites from SQ, highlighting butyrate as a new SQ fermentation product [39].
709 Production of SCFAs, particularly of butyrate, is considered a beneficial function of the gut
710 microbiota and a prominent effect of dietary supplementation with known prebiotics such as
711 resistant starch, inulin-type fructans, and fructooligosaccharides [70–74]. Butyrate is the
712 preferred energy source of the colonocytes [75] and has been linked to the prevention and
713 treatment of colitis [76,77] and colorectal cancer [78]. Supporting the prebiotic potential of
714 SQ, *A. rectalis* maintained stable abundances when switching from a high-fiber to a low-fiber
715 diet supplemented with SQ in a humanized gnotobiotic mouse model colonized with fourteen
716 fiber- and mucin-degrading bacterial strains from the human gut. Without SQ, its abundance
717 dropped approximately 1000-fold after switching to the low-fiber diet. This effect was specific
718 to *A. rectalis* and not observed for *O. symbiosa*, another SQ degrader in the consortium [79].
719

720 The identity and metabolic features of microorganisms involved in SQ degradation in the gut
721 of non-human animals is unknown. Laboratory mice are important models of biomedicine
722 and nutrition research. Here we demonstrate that, similar to the human gut, the capacity for
723 SQ degradation is restricted to few members of the murine microbiota. For example, the
724 sulfofructose-transaldolase pathway, the most prevalent SQ degradation pathway in both
725 systems, is found in only 0.5% of human and 1.1% of mouse gut microbiota species-level
726 genome bins, underscoring its limited distribution (Figure 6) [15]. SQ is mainly degraded via
727 the sulfo-Embden-Meyerhof-Parnas pathway and the sulfofructose-transaldolase pathway to
728 DHPS. Members of the genera *Escherichia* and *Enterocloster* are primary SQ degraders in the
729 mouse gut. The more than 24 h lag phase till onset of SQ degradation in mouse gut content
730 microcosms and the absence of a significant shift in fecal microbiota composition upon single-
731 dose gavage of SQ to mice suggested that microbial SQ metabolism was not active before SQ
732 supplementation. The SQDG contents of mouse chows are not known. However, the absence
733 of SQ in feces before gavaging (Figures 2 h and 5 b) may indicate that the standard mouse
734 chow used in this study, and possibly also in other mouse facilities, is not composed of foods
735 with high SQDG content [3,80,81]. The single 1 mg and 10 mg SQ doses gavaged to mice
736 correspond to the SQ content in approximately 0.37 g and 3.7 g of fresh spinach, which would
737 represent about 7.5% and 75% of the total daily food intake in grams of a mouse, respectively
738 (Table S5). Mice showed no adverse effects after ingesting a high SQ dose. Our results support
739 previous findings from oral SQ supplementation experiments in susceptible IL-10-deficient
740 mice [82]. Daily gavage with 0.45 mg SQ per g body weight, which corresponds roughly to the
741 10 mg SQ dose used in our study, over three weeks did not induce changes in microbial beta-
742 diversity and intestinal inflammation in the IL-10-deficient mice [82].
743

744 Although some mouse microbiota members encode the capacity to either respire DHPS to
745 H_2S (*T. muris*, *Desulfovibrio* species) or ferment DHPS to 3-HPS (*E. clostridioformis*),
746 experiments with gut content microcosms, with conventional laboratory mice, and mouse
747 gut-derived bacterial strains did not provide evidence for active degradation of DHPS. *T. muris*
748 did not utilize DHPS in pure culture [19]. Further, *B. wadsworthia*, a confirmed DHPS degrader
749 in the human gut [15], is not widely distributed among mice and, if present, mostly derived
750 from inoculation of a human strain or human feces transplants [19]. Among the DHPS
751 degradation pathway-encoding taxa in the mouse microbiota, only *E. clostridioformis* was
752 significantly enriched in the mouse gut content microcosms. While we showed that the
753 murine *E. clostridioformis* strain YL32 ferments SQ to DHPS for growth, further degradation
754 of DHPS to 3-HPS was not observed. So-called 'extended sulfoglycolytic pathways' include
755 genes for degradation of SQ and SQ degradation products such as DHPS or sulfolactate [83].
756 For example, *E. gilvus* contains the sulfofructose-transaldolase pathway and the bifurcated
757 HpfGHD-HpfXYZ pathway for SQ and DHPS degradation [18]. *F. prausnitzii* is thought to also
758 possess an extended sulfoglycolytic pathway, as its genome encodes the sulfofructose-
759 transaldolase pathway along with a putative *hpfG* [17]. The HpfGHD pathway and the HpfXYZ
760 pathway both do not produce H_2S from DHPS [17,18]. The HpfGHD pathway does not
761 conserve energy, but regenerates NAD^+ [17], while ATP is generated in the bifurcated HpfXYZ
762 pathway [18]. Our results indicate that DHPS is not a relevant growth substrate for the gut
763 microbiota of conventional laboratory mice. Unlike the human gut, where SQ degradation
764 proceeds beyond DHPS, SQ degradation stopped at the level of DHPS in the mouse gut and
765 did not contribute to sulfide production. However, a previous study reported significant
766 sulfide production after 168 h incubation of anoxic microcosms with feces of IL-10-deficient
767 mice and 4 mM SQ, which indicated complete SQ degradation by the microbiota of this mouse

768 model [82]. Microbiota composition was not analyzed in the fecal microcosms of IL-10-
769 deficient mice. Yet, the discrepancy between the findings of this previous study and our study
770 may be attributed to differences in microbial community structure and in incubation times.
771 H_2S-producing bacteria of the family *Desulfovibrionaceae* (genera *Taurinivorans*,
772 *Desulfovibrio*, and *Mailhella*) seem to be generally more abundant in wild mice compared to
773 laboratory mice [19,28,84]. Whether the absence of an active DHPS metabolism observed in
774 the laboratory mice in our study reflects a host-specific microbial adaptation that is conserved
775 across diverse wild and laboratory mouse lineages [85] or results from the specific diet and
776 housing of laboratory mice remains unclear.
777
778

779 Conclusions

780 Our work demonstrates that dietary SQ is exclusively degraded by the gut microbiota and not
781 directly metabolized by the human and murine host. We observed the enrichment of
782 commensal bacteria and significantly increased acetate and butyrate production in human
783 fecal microcosms at high physiological SQ concentrations. These results align with key criteria
784 for prebiotics [70]. SQ degradation by the gut microbiota of conventional wild type laboratory
785 mice differed fundamentally from humans, primarily by the lack of DHPS degradation.
786 Gnotobiotic animals colonized with defined consortia of microbial strains, including primary
787 and secondary SQ degraders, may be better models to study effects of complete SQ
788 degradation on the host [79,82]. Our study provides fundamental insight into SQ degradation

789 in the mammalian gut, and has implications for potential application of SQDG-containing
790 foods or SQ in dietary and prebiotic interventions.
791

792 # Declarations

793 ## Ethics approval and consent to participate

794 Sampling and microbial analyses of feces from healthy human adults was approved by the
795 ethics committee of the University of Vienna, Austria (reference numbers 00161 and 00714).
796 Experiments with wild type mice were approved by the national authorities in Austria
797 (Bundesministerium für Bildung, Wissenschaft und Forschung, 2022-0.745.974). Experiments
798 with germ-free mice were approved by the local authorities in Germany (Regierung von
799 Oberbayern, ROB-55.2-2532.Vet_02-19-53).

800 ## Consent for publication

801 Not applicable.

802 ## Availability of data and material

803 All sequence data generated in this project is available at NCBI under BioProject ID
804 PRJNA1198716. The hidden Markov models developed in this project (Table S1) are available
805 as Additional File 1.

806 ## Competing interests

807 The authors declare that they have no competing interests.

Funding

This research was funded by the Austrian Science Fund (FWF) [grant DOI 10.55776/DOC69 and 10.55776/COE7]. For open access purposes, the authors have applied for a CC BY public copyright license to any author-accepted manuscript version arising from this submission. BS received funding from the DFG (project no. 395357507 “SFB1371”), the European Research Council (EvoGutHealth, 865615), and the Germany Centre for Infection Research (project no. 503-5-7-06.712_00 and 503-5-7-06.709_00).

Authors' contributions

J.K. and A.L. conceived the study. J.K., B.T.H., A.S.W., S.B., M.L., and G.A. performed experiments and analyzed data. A.R., D.B., D.M., D.S., and B.S. contributed essential experimental infrastructure and analytical instrumentation, and expert advice. J.K., T.S.T., and B.H. performed bioinformatic analyses. J.K., B.T.H., A.S.W., S.B., T.S.T., M.M., and A.L. interpreted the data. J.K., M.M., and A.L. wrote the article. All authors revised and approved the manuscript.

Acknowledgements

We thank the staff of the Joint Microbiome Facility for sequencing and Margarete Watzka for isotope ratio mass spectrometry measurements.

826 # References

827 1. Harwood JL, Nicholls RG. The plant sulpholipid—a major component of the sulphur cycle.
828 Biochem Soc Trans. 1979;7:440–7.

829 2. Snow AJD, Burchill L, Sharma M, Davies GJ, Williams SJ. Sulfoglycolysis: catabolic pathways
830 for metabolism of sulfoquinovose. Chem Soc Rev. 2021;50:13628–45.

831 3. Goddard-Borger ED, Williams SJ. Sulfoquinovose in the biosphere: occurrence, metabolism
832 and functions. Biochem J. 2017;474:827–49.

833 4. Sato N, Aoki M, Maru Y, Sonoike K, Minoda A, Tsuzuki M. Involvement of sulfoquinovosyl
834 diacylglycerol in the structural integrity and heat-tolerance of photosystem II. Planta.
835 2003;217:245–51.

836 5. Nakajima Y, Umena Y, Nagao R, Endo K, Kobayashi K, Akita F, *et al*. Thylakoid membrane
837 lipid sulfoquinovosyl-diacylglycerol (SQDG) is required for full functioning of photosystem II
838 in *Thermosynechococcus elongatus*. J Biol Chem. 2018;293:14786–97.

839 6. Speciale G, Jin Y, Davies GJ, Williams SJ, Goddard-Borger ED. YihQ is a sulfoquinovosidase
840 that cleaves sulfoquinovosyl diacylglyceride sulfolipids. Nat Chem Biol. 2016;12:215–7.

841 7. Kaur A, Pickles IB, Sharma M, Madeido Soler N, Scott NE, Pidot SJ, *et al*. Widespread family
842 of NAD+-dependent sulfoquinovosidases at the gateway to sulfoquinovose catabolism. J Am
843 Chem Soc. 2023;145:28216–23.

844 8. Sharma M, Lingford JP, Petricevic M, Snow AJD, Zhang Y, Järvå MA, *et al*. Oxidative
845 desulfurization pathway for complete catabolism of sulfoquinovose by bacteria. Proc Natl
846 Acad Sci USA. 2022;119.

847 9. Ye Z, Wei Y, Jiang L, Zhang Y. Oxygenolytic sulfoquinovose degradation by an iron-
848 dependent alkanesulfonate dioxygenase. iScience. 2023;26:107803.

849 10. Denger K, Weiss M, Felux A-K, Schneider A, Mayer C, Spiteller D, *et al*. Sulphoglycolysis in
850 *Escherichia coli* K-12 closes a gap in the biogeochemical sulphur cycle. Nature. 2014;507:114–
851 7.

852 11. Liu J, Wei Y, Ma K, An J, Liu X, Liu Y, *et al*. Mechanistically diverse pathways for
853 sulfoquinovose degradation in bacteria. ACS Catal. 2021;11:14740–50.

854 12. Felux A-K, Spiteller D, Klebensberger J, Schleheck D. Entner-Doudoroff pathway for
855 sulfoquinovose degradation in *Pseudomonas putida* SQ1. Proc Natl Acad Sci USA.
856 2015;112:E4298-305.

857 13. Frommeyer B, Fiedler AW, Oehler SR, Hanson BT, Loy A, Franchini P, *et al*. Environmental
858 and intestinal phylum Firmicutes bacteria metabolize the plant sugar sulfoquinovose via a 6-
859 deoxy-6-sulfofructose transaldolase pathway. iScience. 2020;23:101510.

860 14. Liu Y, Wei Y, Zhou Y, Ang EL, Zhao H, Zhang Y. A transaldolase-dependent sulfoglycolysis
861 pathway in *Bacillus megaterium* DSM 1804. Biochem Biophys Res Commun. 2020;533:1109–
862 14.

863 15. Hanson BT, Dimitri Kits K, Löffler J, Burrichter AG, Fiedler A, Denger K, *et al*. Sulfoquinovose
864 is a select nutrient of prominent bacteria and a source of hydrogen sulfide in the human gut.
865 ISME J. 2021;15:2779–91.

866 16. Burrichter A, Denger K, Franchini P, Huhn T, Müller N, Spiteller D, *et al*. Anaerobic
867 degradation of the plant sugar sulfoquinovose concomitant with H_2S production: *Escherichia*
868 *coli* K-12 and *Desulfovibrio* sp. strain DF1 as co-culture model. Front Microbiol. 2018;9:2792.

869 17. Liu J, Wei Y, Lin L, Teng L, Yin J, Lu Q, *et al*. Two radical-dependent mechanisms for
870 anaerobic degradation of the globally abundant organosulfur compound
871 dihydroxypropanesulfonate. Proc Natl Acad Sci USA. 2020;117:15599–608.

872 18. Chen Y, Chu R, Ma K, Jiang L, Yang Q, Li Z, *et al*. Study of sulfoglycolysis in *Enterococcus*
873 *gilvus* reveals a widespread bifurcated pathway for dihydroxypropanesulfonate degradation.
874 iScience. 2024;111010.

875 19. Ye H, Borusak S, Eberl C, Krasenbrink J, Weiss AS, Chen S-C, *et al*. Ecophysiology and
876 interactions of a taurine-respiring bacterium in the mouse gut. Nat Commun. 2023;14:5533.

877 20. Mayer J, Huhn T, Habeck M, Denger K, Hollemeyer K, Cook AM. 2,3-Dihydroxypropane-1-
878 sulfonate degraded by *Cupriavidus pinatubonensis* JMP134: purification of
879 dihydroxypropanesulfonate 3-dehydrogenase. Microbiology. 2010;156:1556–64.

880 21. Denger K, Cook AM. Racemase activity effected by two dehydrogenases in sulfolactate
881 degradation by *Chromohalobacter salexigens*: purification of (S)-sulfolactate dehydrogenase.
882 Microbiology. 2010;156:967–74.

883 22. Pasolli E, Asnicar F, Manara S, Zolfo M, Karcher N, Armanini F, *et al*. Extensive unexplored
884 human microbiome diversity revealed by over 150,000 genomes from metagenomes
885 spanning age, geography, and lifestyle. Cell. 2019;176:649-662.e20.

886 23. Dikeocha IJ, Al-Kabsi AM, Chiu H-T, Alshawsh MA. *Faecalibacterium prausnitzii*
887 ameliorates colorectal tumorigenesis and suppresses proliferation of HCT116 colorectal
888 cancer cells. Biomedicines. 2022;10:1128.

889 24. Zeevi D, Korem T, Zmora N, Israeli D, Rothschild D, Weinberger A, *et al*. Personalized
890 nutrition by prediction of glycemic responses. Cell. 2015;163:1079–94.

891 25. Banerjee R. Hydrogen sulfide: redox metabolism and signaling. Antioxid Redox Signal.
892 2011;15:339–41.

893 26. Blachier F, Beaumont M, Kim E. Cysteine-derived hydrogen sulfide and gut health: a
894 matter of endogenous or bacterial origin. Curr Opin Clin Nutr Metab Care. 2019;22:68–75.

895 27. Olson KR, Straub KD. The role of hydrogen sulfide in evolution and the evolution of

896 hydrogen sulfide in metabolism and signaling. Physiology . 2016;31:60–72.

897 28. Stacy A, Andrade-Oliveira V, McCulloch JA, Hild B, Oh JH, Perez-Chaparro PJ, *et al*. Infection
898 trains the host for microbiota-enhanced resistance to pathogens. Cell. 2021;184:615-627.e17.

899 29. Ijssennagger N, Belzer C, Hooiveld GJ, Dekker J, van Mil SWC, Müller M, *et al*. Gut
900 microbiota facilitates dietary heme-induced epithelial hyperproliferation by opening the
901 mucus barrier in colon. Proc Natl Acad Sci USA. 2015;112:10038–43.

902 30. Beauchamp RO Jr, Bus JS, Popp JA, Boreiko CJ, Andjelkovich DA. A critical review of the
903 literature on hydrogen sulfide toxicity. Crit Rev Toxicol. 1984;13:25–97.

904 31. Devkota S, Wang Y, Musch MW, Leone V, Fehlner-Peach H, Nadimpalli A, *et al*. Dietary-
905 fat-induced taurocholic acid promotes pathobiont expansion and colitis in Il10-/- mice.
906 Nature. 2012;487:104–8.

907 32. Carbonero F, Benefiel AC, Alizadeh-Ghamsari AH, Gaskins HR. Microbial pathways in
908 colonic sulfur metabolism and links with health and disease. Front Physiol. 2012;3:448.

909 33. Vichai V, Kirtikara K. Sulforhodamine B colorimetric assay for cytotoxicity screening. Nat
910 Protoc. 2006;1:1112–6.

911 34. Brugiroux S, Beutler M, Pfann C, Garzetti D, Ruscheweyh H-J, Ring D, *et al*. Genome-guided
912 design of a defined mouse microbiota that confers colonization resistance against *Salmonella*
913 *enterica* serovar Typhimurium. Nat Microbiol. 2016;2:16215.

914 35. Gronbach K, Flade I, Holst O, Lindner B, Ruscheweyh HJ, Wittmann A, *et al*. Endotoxicity
915 of lipopolysaccharide as a determinant of T-cell-mediated colitis induction in mice.
916 Gastroenterology. 2014;146:765–75.

917 36. Zhang Y, Mui JW-Y, Arumaperuma T, Lingford JP, Goddard-Borger ED, White JM, *et al*.
918 Concise synthesis of sulfoquinovose and sulfoquinovosyl diacylglycerides, and development
919 of a fluorogenic substrate for sulfoquinovosidases. Org Biomol Chem. 2020;18:675–86.

920 37. FELASA working group on revision of guidelines for health monitoring of rodents and
921 rabbits, Mähler Convenor M, Berard M, Feinstein R, Gallagher A, Illgen-Wilcke B, *et al*. FELASA
922 recommendations for the health monitoring of mouse, rat, hamster, guinea pig and rabbit
923 colonies in breeding and experimental units. Lab Anim. 2014;48:178–92.

924 38. Cline JD. Spectrophotometric determination of hydrogen sulfide in natural waters. Limnol
925 Oceanogr. 1969;14:454–8.

926 39. Borusak S, Denger K, Dorendorf T, Fournier C, Lerner H, Mayans O, *et al*. Anaerobic
927 *Faecalicatena* spp. degrade sulfoquinovose via a bifurcated 6-deoxy-6-sulfofructose
928 transketolase/transaldolase pathway to both C2- and C3-sulfonate intermediates. Front
929 Microbiol. 2024;15:1491101.

930 40. Pjevac P, Hausmann B, Schwarz J, Kohl G, Herbold CW, Loy A, *et al*. An economical and
931 flexible dual barcoding, two-step PCR approach for highly multiplexed amplicon sequencing.

932 Front Microbiol. 2021;12:669776.

933 41. Herbold CW, Pelikan C, Kuzyk O, Hausmann B, Angel R, Berry D, *et al*. A flexible and
934 economical barcoding approach for highly multiplexed amplicon sequencing of diverse target
935 genes. Front Microbiol. 2015;6:731.

936 42. Callahan BJ, McMurdie PJ, Rosen MJ, Han AW, Johnson AJA, Holmes SP. DADA2: High-
937 resolution sample inference from Illumina amplicon data. Nat Methods. 2016;13:581–3.

938 43. McMurdie PJ, Holmes S. phyloseq: an R package for reproducible interactive analysis and
939 graphics of microbiome census data. PLoS One. 2013;8:e61217.

940 44. Oksanen J. vegan : Community Ecology Package-R package version 1.17-8. http://CRANR-
941 project.org/package=vegan. 2011. Accessed 12 Jun 2024.

942 45. Love MI, Huber W, Anders S. Moderated estimation of fold change and dispersion for RNA-
943 seq data with DESeq2. Genome Biol. 2014;15:550.

944 46. Sayers EW, Bolton EE, Brister JR, Canese K, Chan J, Comeau DC, *et al*. Database resources
945 of the national center for biotechnology information. Nucleic Acids Res. 2022;50:D20–6.

946 47. Parada AE, Needham DM, Fuhrman JA. Every base matters: assessing small subunit rRNA
947 primers for marine microbiomes with mock communities, time series and global field
948 samples. Environ Microbiol. 2016;18:1403–14.

949 48. Apprill A, McNally S, Parsons R, Weber L. Minor revision to V4 region SSU rRNA 806R gene
950 primer greatly increases detection of SAR11 bacterioplankton. Aquat Microb Ecol.
951 2015;75:129–37.

952 49. Beresford-Jones BS, Forster SC, Stares MD, Notley G, Viciani E, Browne HP, *et al*. The
953 Mouse Gastrointestinal Bacteria Catalogue enables translation between the mouse and
954 human gut microbiotas via functional mapping. Cell Host Microbe. 2022;30:124-138.e8.

955 50. Tanabe TS, Dahl C. HMSS2: An advanced tool for the analysis of sulphur metabolism,
956 including organosulphur compound transformation, in genome and metagenome assemblies.
957 Mol Ecol Resour. 2023;23:1930–45.

958 51. Tanabe TS, Dahl C. HMS-S-S: A tool for the identification of Sulphur metabolism-related
959 genes and analysis of operon structures in genome and metagenome assemblies. Mol Ecol
960 Resour. 2022;22:2758–74.

961 52. Morimoto Y, Uesaka K, Fujita Y, Yamamoto H. A nitrogenase-like enzyme is involved in the
962 novel anaerobic assimilation pathway of a sulfonate, isethionate, in the photosynthetic
963 bacterium *Rhodobacter capsulatus*. mSphere. 2024;9:e00498-24.

964 53. An J, Wei Y, Liu J, Lui Ang E, Zhao H, Zhang Y. Biochemical investigation of 3-
965 sulfopropionaldehyde reductase HpfD. Chembiochem. 2021;22:2862–6.

966 54. Svetlitsky D, Dagan T, Ziv-Ukelson M. Discovery of multi-operon colinear syntenic blocks
967 in microbial genomes. Bioinformatics. 2020;36:i21–9.

968 55. Vander Heiden MG, Locasale JW, Swanson KD, Sharfi H, Heffron GJ, Amador-Noguez D, *et*
969 *al*. Evidence for an alternative glycolytic pathway in rapidly proliferating cells. Science.
970 2010;329:1492–9.

971 56. Gupta SD, Sastry PS. Metabolism of the plant sulfolipid--sulfoquinovosyldiacylglycerol:
972 degradation in animal tissues. Arch Biochem Biophys. 1987;259:510–9.

973 57. Andersson L, Bratt C, Arnoldsson KC, Herslöf B, Olsson NU, Sternby B, *et al*. Hydrolysis of
974 galactolipids by human pancreatic lipolytic enzymes and duodenal contents. J Lipid Res.
975 1995;36:1392–400.

976 58. Benson AA, Lee RF. The sulphoglycolytic pathway in plants. Biochem J. 1972;128:29P-30P.

977 59. Roy AB, Hewlins MJE, Ellis AJ, Harwood JL, White GF. Glycolytic breakdown of
978 sulfoquinovose in bacteria: a missing link in the sulfur cycle. Appl Environ Microbiol.
979 2003;69:6434–41.

980 60. Scholz S, Serif M, Schleheck D, Sayer MDJ, Cook AM, Küpper FC. Sulfoquinovose
981 metabolism in marine algae. Botanica Marina. 2021;64:301–12.

982 61. Kuriyama I, Musumi K, Yonezawa Y, Takemura M, Maeda N, Iijima H, *et al*. Inhibitory
983 effects of glycolipids fraction from spinach on mammalian DNA polymerase activity and
984 human cancer cell proliferation. J Nutr Biochem. 2005;16:594–601.

985 62. Sharma M, Abayakoon P, Epa R, Jin Y, Lingford JP, Shimada T, *et al*. Molecular basis of
986 sulfosugar selectivity in sulfoglycolysis. ACS Cent Sci. 2021;7:476–87.

987 63. Fu X, Liu Z, Zhu C, Mou H, Kong Q. Nondigestible carbohydrates, butyrate, and butyrate-
988 producing bacteria. Crit Rev Food Sci Nutr. 2019;59:S130–52.

989 64. Sakamoto M, Hisatomi A, Ohkuma M. Isolation and characterization of a novel *Waltera*
990 species and reclassification of *Brotolimicola acetigignens* Hitch *et al*. 2022 as *Waltera*
991 *acetigignens* comb. nov. Int J Syst Evol Microbiol. 2024;74:006381.

992 65. Van-Wehle T, Vital M. Investigating the response of the butyrate production potential to
993 major fibers in dietary intervention studies. NPJ Biofilms Microbiomes. 2024;10:63.

994 66. Barcenilla A, Pryde SE, Martin JC, Duncan SH, Stewart CS, Henderson C, *et al*. Phylogenetic
995 relationships of butyrate-producing bacteria from the human gut. Appl Environ Microbiol.
996 2000;66:1654–61.

997 67. Duncan SH, Barcenilla A, Stewart CS, Pryde SE, Flint HJ. Acetate utilization and butyryl
998 coenzyme A (CoA):acetate-CoA transferase in butyrate-producing bacteria from the human
999 large intestine. Appl Environ Microbiol. 2002;68:5186–90.

1000 68. Louis P, Young P, Holtrop G, Flint HJ. Diversity of human colonic butyrate-producing
1001 bacteria revealed by analysis of the butyryl-CoA:acetate CoA-transferase gene. Environ
1002 Microbiol. 2010;12:304–14.

1003 69. Louis P, Duncan SH, McCrae SI, Millar J, Jackson MS, Flint HJ. Restricted distribution of the
1004 butyrate kinase pathway among butyrate-producing bacteria from the human colon. Journal
1005 of Bacteriology. 2004; 186(7):2099-106.

1006 70. Hutkins R, Walter J, Gibson GR, Bedu-Ferrari C, Scott K, Tancredi DJ, *et al*. Classifying
1007 compounds as prebiotics - scientific perspectives and recommendations. Nat Rev
1008 Gastroenterol Hepatol. 2024;1–17.

1009 71. DeMartino P, Cockburn DW. Resistant starch: impact on the gut microbiome and health.
1010 Curr Opin Biotechnol. 2020;61:66–71.

1011 72. Timm DA, Stewart ML, Hospattankar A, Slavin JL. Wheat dextrin, psyllium, and inulin
1012 produce distinct fermentation patterns, gas volumes, and short-chain fatty acid profiles in
1013 vitro. J Med Food. 2010;13:961–6.

1014 73. Roberfroid MB. Introducing inulin-type fructans. Br J Nutr. 2005;93 Suppl 1:S13-25.

1015 74. Hosoya N, Dhorranintra B, Hidaka H. Utilization of [U-^{14}C]fructooligosaccharides in man as
1016 energy resources. Journal of Clinical Biochemistry and Nutrition. 1988;5:67–74.

1017 75. Hodgkinson K, El Abbar F, Dobranowski P, Manoogian J, Butcher J, Figeys D, *et al*.
1018 Butyrate's role in human health and the current progress towards its clinical application to
1019 treat gastrointestinal disease. Clin Nutr. 2023;42:61–75.

1020 76. Recharla N, Geesala R, Shi X-Z. Gut microbial metabolite butyrate and its therapeutic role
1021 in inflammatory bowel disease: A literature review. Nutrients. 2023;15(10):2275.

1022 77. Segain JP, Raingeard de la Blétière D, Bourreille A, Leray V, Gervois N, Rosales C, *et al*.
1023 Butyrate inhibits inflammatory responses through NFkappaB inhibition: implications for
1024 Crohn's disease. Gut. 2000;47:397–403.

1025 78. Kang J, Sun M, Chang Y, Chen H, Zhang J, Liang X, *et al*. Butyrate ameliorates colorectal
1026 cancer through regulating intestinal microecological disorders. Anticancer Drugs.
1027 2023;34:227–37.

1028 79. Sharma M, Pudlo N, Järvå MA, Kaur A, John A, Burchill L, *et al*. Sulfoglycolysis sustains
1029 *Eubacterium rectale* in low-fiber diets. J Biol Chem. 2025;108320.

1030 80. Weidmann E, Samadi N, Klems M, Heiden D, Seppova K, Ret D, *et al*. Mouse chow
1031 composition influences immune responses and food allergy development in a mouse model.
1032 Nutrients. 2018;10:1775.

1033 81. Whelan J, Whelan J. Conversion of dietary polyunsaturated fats between humans and
1034 rodents: A review of allometric scaling models. Prostaglandins Leukot Essent Fatty Acids.
1035 2020;158:102094.

1036 82. Burkhardt W, Rausch T, Klopfleisch R, Blaut M, Braune A. Impact of dietary sulfolipid-
1037 derived sulfoquinovose on gut microbiota composition and inflammatory status of colitis-
1038 prone interleukin-10-deficient mice. Int J Med Microbiol. 2021;311:151494.

1039 83. Wei Y, Tong Y, Zhang Y. New mechanisms for bacterial degradation of sulfoquinovose.
1040 Biosci Rep. 2022;42(10):BSR20220314.

1041 84. Rosshart SP, Herz J, Vassallo BG, Hunter A, Wall MK, Badger JH, *et al*. Laboratory mice born
1042 to wild mice have natural microbiota and model human immune responses. Science.
1043 2019;365:eaaw4361.

1044 85. Sprockett DD, Dillard BA, Landers AA, Sanders JG, Moeller AH. Recent genetic drift in the
1045 co-diversified gut bacterial symbionts of laboratory mice. Nat Commun. 2025;16:2218.

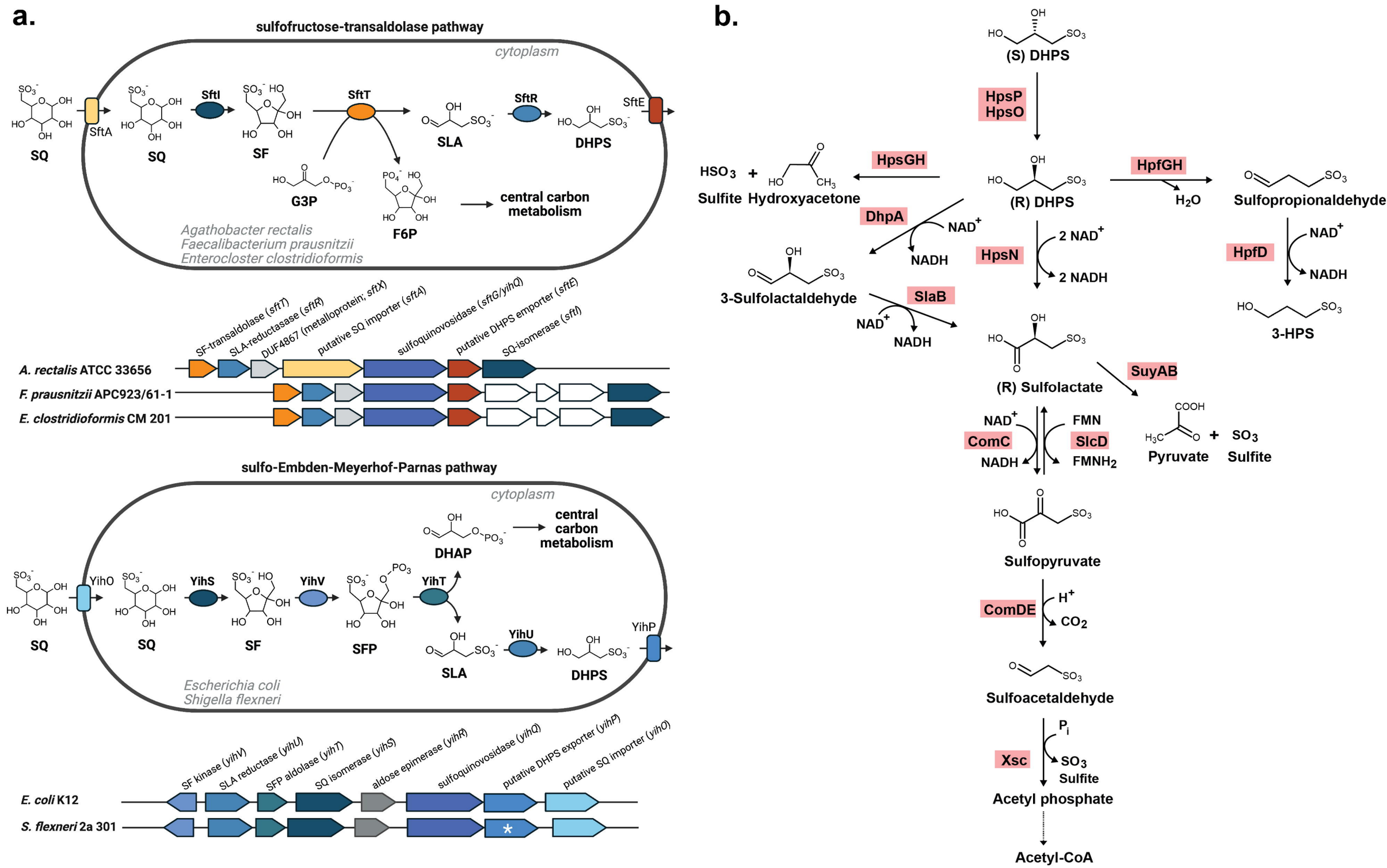
a.
sulfofructose-transaldolase pathway
cytoplasm
SQ
SftA
SQ
SftI
SF
SftT
SLA
SftR
DHPS
SftE
G3P
F6P
central carbon metabolism
Agathobacter rectalis
Faecalibacterium prausnitzii
Enterocloster clostridioformis
SF-transaldolase (sftT)
SLA-reductasase (sftR)
DUF4867 (metalloprotein; sftX)
putative SQ importer (sftA)
sulfoquinovosidase (sftG/yihQ)
putative DHPS emporter (sftE)
SQ-isomerase (sftI)
A. rectalis ATCC 33656
F. prausnitzii APC923/61-1
E. clostridioformis CM 201
sulfo-Embden-Meyerhof-Parnas pathway
cytoplasm
DHAP
central carbon metabolism
SQ
YihO
SQ
YihS
SF
YihV
SFP
YihT
SLA
YihU
DHPS
YihP
Escherichia coli
Shigella flexneri
SF kinase (yihV)
SLA reductase (yihU)
SFP aldolase (yihT)
SQ isomerase (yihS)
aldose epimerase (yihR)
sulfoquinovosidase (yihQ)
putative DHPS exporter (yihP)
putative SQ importer (yihO)
E. coli K12
S. flexneri 2a 301
b.
(S) DHPS
HpsP
HpsO
HpsGH
HSO3 + Sulfite
Hydroxyacetone
(R) DHPS
HpfGH
H2O
Sulfopropionaldehyde
DhpA
NAD+
NADH
HpsN
2 NAD+
2 NADH
HpfD
NAD+
NADH
3-HPS
3-Sulfolactaldehyde
SlaB
NAD+
NADH
(R) Sulfolactate
SuyAB
NAD+
ComC
NADH
FMN
SlcD
FMNH2
Pyruvate
+ SO3
Sulfite
Sulfopyruvate
ComDE
H+
CO2
Sulfoacetaldehyde
Pi
Xsc
SO3
Sulfite
Acetyl phosphate
Acetyl-CoA

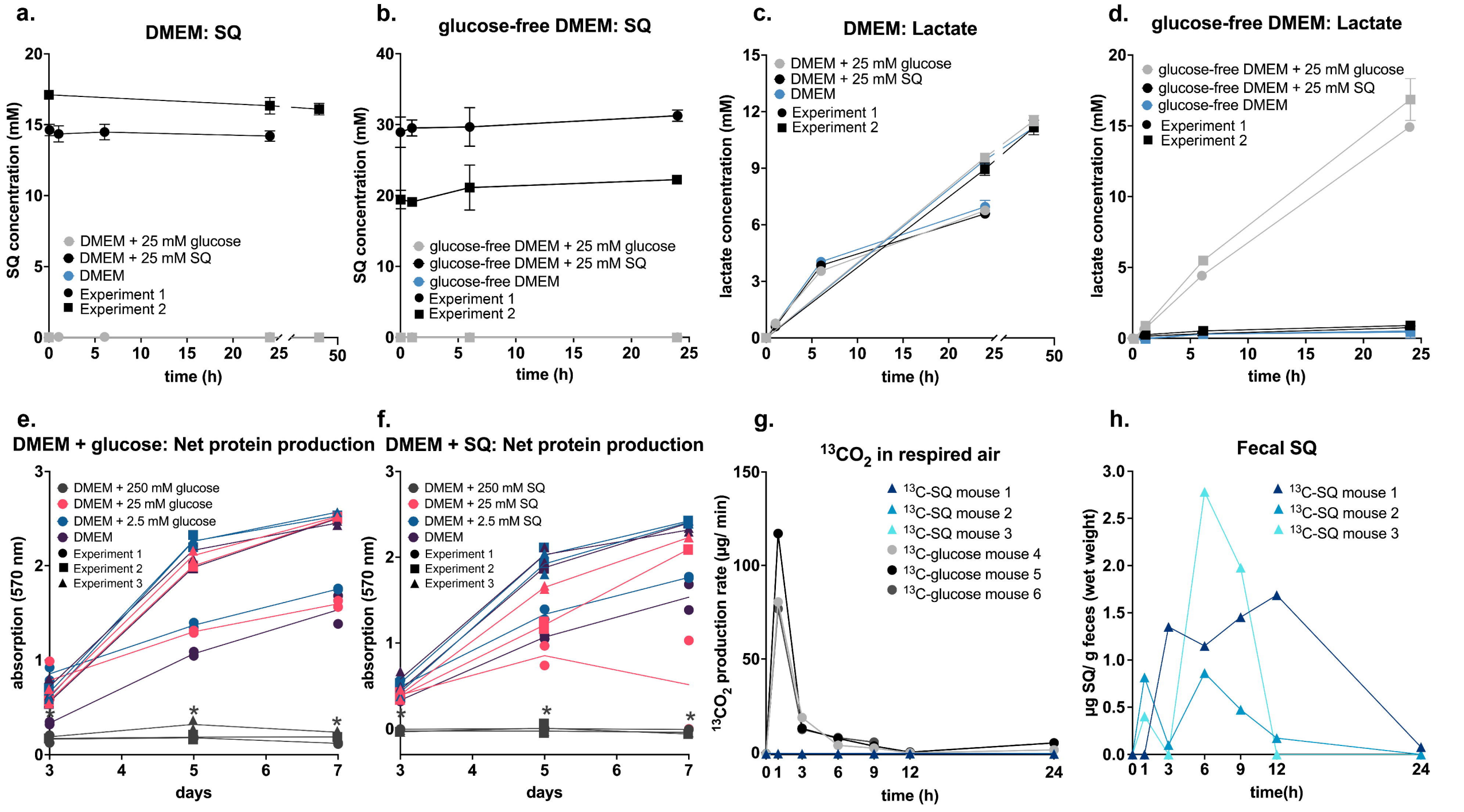
a.
DMEM: SQ
SQ concentration (mM)
time (h)
DMEM + 25 mM glucose
DMEM + 25 mM SQ
DMEM
Experiment 1
Experiment 2
b.
glucose-free DMEM: SQ
SQ concentration (mM)
time (h)
glucose-free DMEM + 25 mM glucose
glucose-free DMEM + 25 mM SQ
glucose-free DMEM
Experiment 1
Experiment 2
c.
DMEM: Lactate
lactate concentration (mM)
time (h)
DMEM + 25 mM glucose
DMEM + 25 mM SQ
DMEM
Experiment 1
Experiment 2
d.
glucose-free DMEM: Lactate
lactate concentration (mM)
time (h)
glucose-free DMEM + 25 mM glucose
glucose-free DMEM + 25 mM SQ
glucose-free DMEM
Experiment 1
Experiment 2
e.
DMEM + glucose: Net protein production
absorption (570 nm)
days
DMEM + 250 mM glucose
DMEM + 25 mM glucose
DMEM + 2.5 mM glucose
DMEM
Experiment 1
Experiment 2
Experiment 3
f.
DMEM + SQ: Net protein production
absorption (570 nm)
days
DMEM + 250 mM SQ
DMEM + 25 mM SQ
DMEM + 2.5 mM SQ
DMEM
Experiment 1
Experiment 2
Experiment 3
g.
$^{13}CO_2$ in respired air
$^{13}CO_2$ production rate (µg/ min)
time (h)
^{13}C-SQ mouse 1
^{13}C-SQ mouse 2
^{13}C-SQ mouse 3
^{13}C-glucose mouse 4
^{13}C-glucose mouse 5
^{13}C-glucose mouse 6
h.
Fecal SQ
µg SQ/ g feces (wet weight)
time(h)
^{13}C-SQ mouse 1
^{13}C-SQ mouse 2
^{13}C-SQ mouse 3

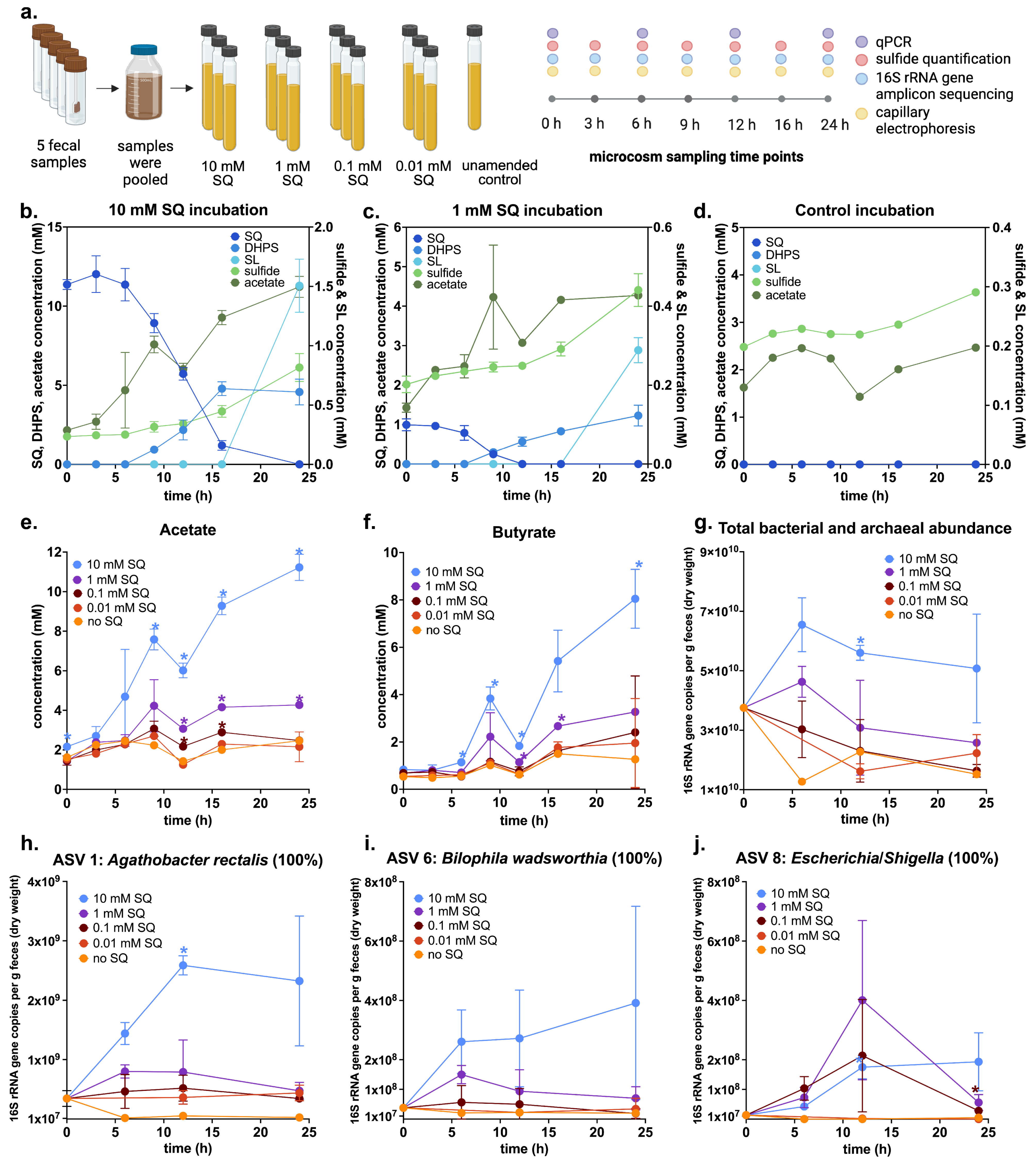
a.
5 fecal samples
samples were pooled
10 mM SQ
1 mM SQ
0.1 mM SQ
0.01 mM SQ
unamended control
0 h
3 h
6 h
9 h
12 h
16 h
24 h
qPCR
sulfide quantification
16S rRNA gene amplicon sequencing
capillary electrophoresis
microcosm sampling time points
b.
10 mM SQ incubation
c.
1 mM SQ incubation
d.
Control incubation
SQ
DHPS
SL
sulfide
acetate
SQ, DHPS, acetate concentration (mM)
sulfide & SL concentration (mM)
time (h)
e.
Acetate
f.
Butyrate
g.
Total bacterial and archaeal abundance
10 mM SQ
1 mM SQ
0.1 mM SQ
0.01 mM SQ
no SQ
concentration (mM)
16S rRNA gene copies per g feces (dry weight)
h.
ASV 1: Agathobacter rectalis (100%)
i.
ASV 6: Bilophila wadsworthia (100%)
j.
ASV 8: Escherichia/Shigella (100%)

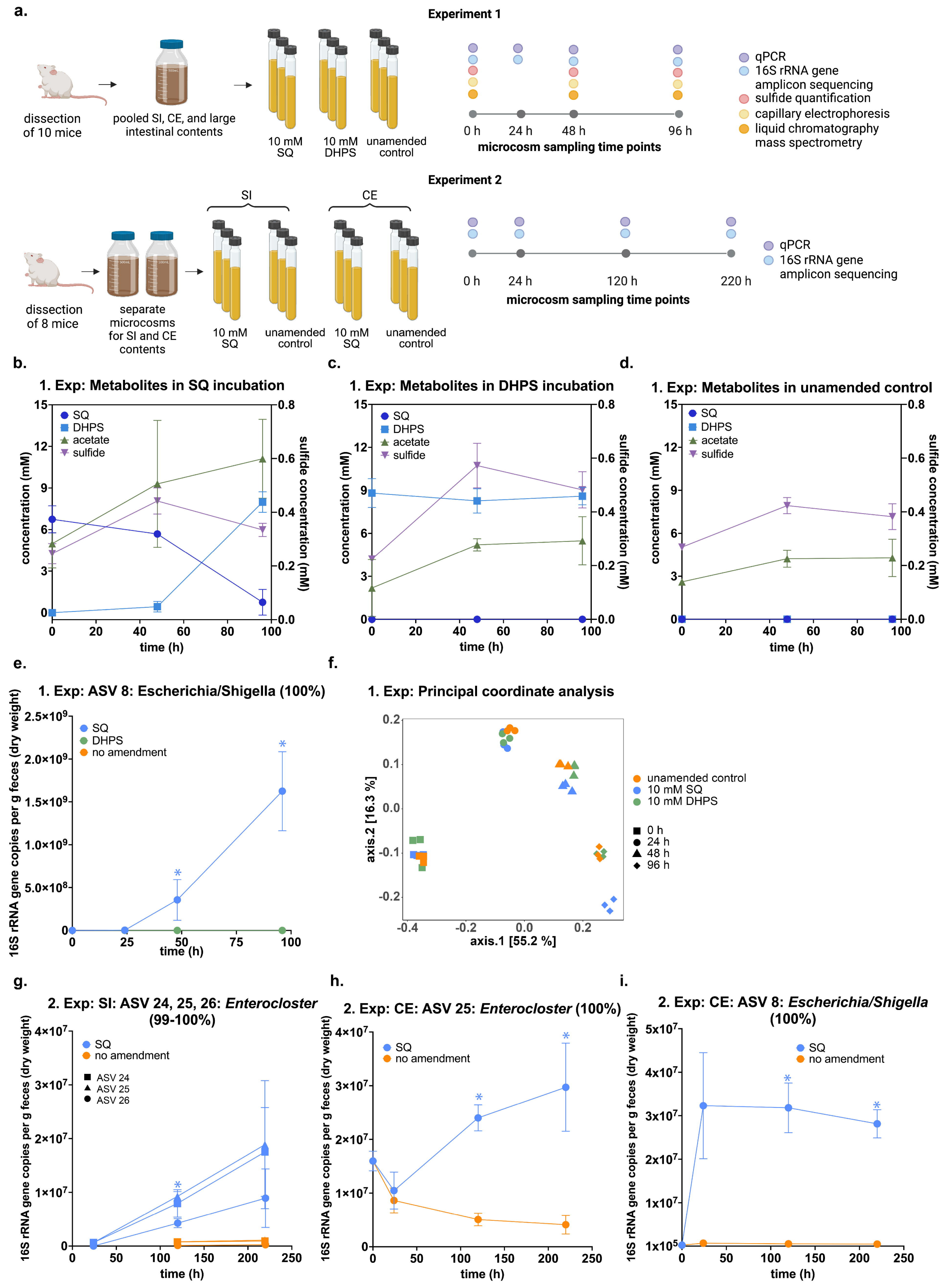
a.
Experiment 1
dissection of 10 mice
pooled SI, CE, and large intestinal contents
10 mM SQ
10 mM DHPS
unamended control
0 h
24 h
48 h
96 h
microcosm sampling time points
qPCR
16S rRNA gene amplicon sequencing
sulfide quantification
capillary electrophoresis
liquid chromatography mass spectrometry
Experiment 2
SI
CE
dissection of 8 mice
separate microcosms for SI and CE contents
10 mM SQ
unamended control
10 mM SQ
unamended control
0 h
24 h
120 h
220 h
microcosm sampling time points
qPCR
16S rRNA gene amplicon sequencing
b.
1. Exp: Metabolites in SQ incubation
c.
1. Exp: Metabolites in DHPS incubation
d.
1. Exp: Metabolites in unamended control
SQ
DHPS
acetate
sulfide
concentration (mM)
sulfide concentration (mM)
time (h)
e.
f.
1. Exp: ASV 8: Escherichia/Shigella (100%)
SQ
DHPS
no amendment
16S rRNA gene copies per g feces (dry weight)
time (h)
1. Exp: Principal coordinate analysis
unamended control
10 mM SQ
10 mM DHPS
0 h
24 h
48 h
96 h
axis.2 [16.3 %]
axis.1 [55.2 %]
g.
h.
i.
2. Exp: SI: ASV 24, 25, 26: Enterocloster (99-100%)
ASV 24
ASV 25
ASV 26
2. Exp: CE: ASV 25: Enterocloster (100%)
2. Exp: CE: ASV 8: Escherichia/Shigella (100%)

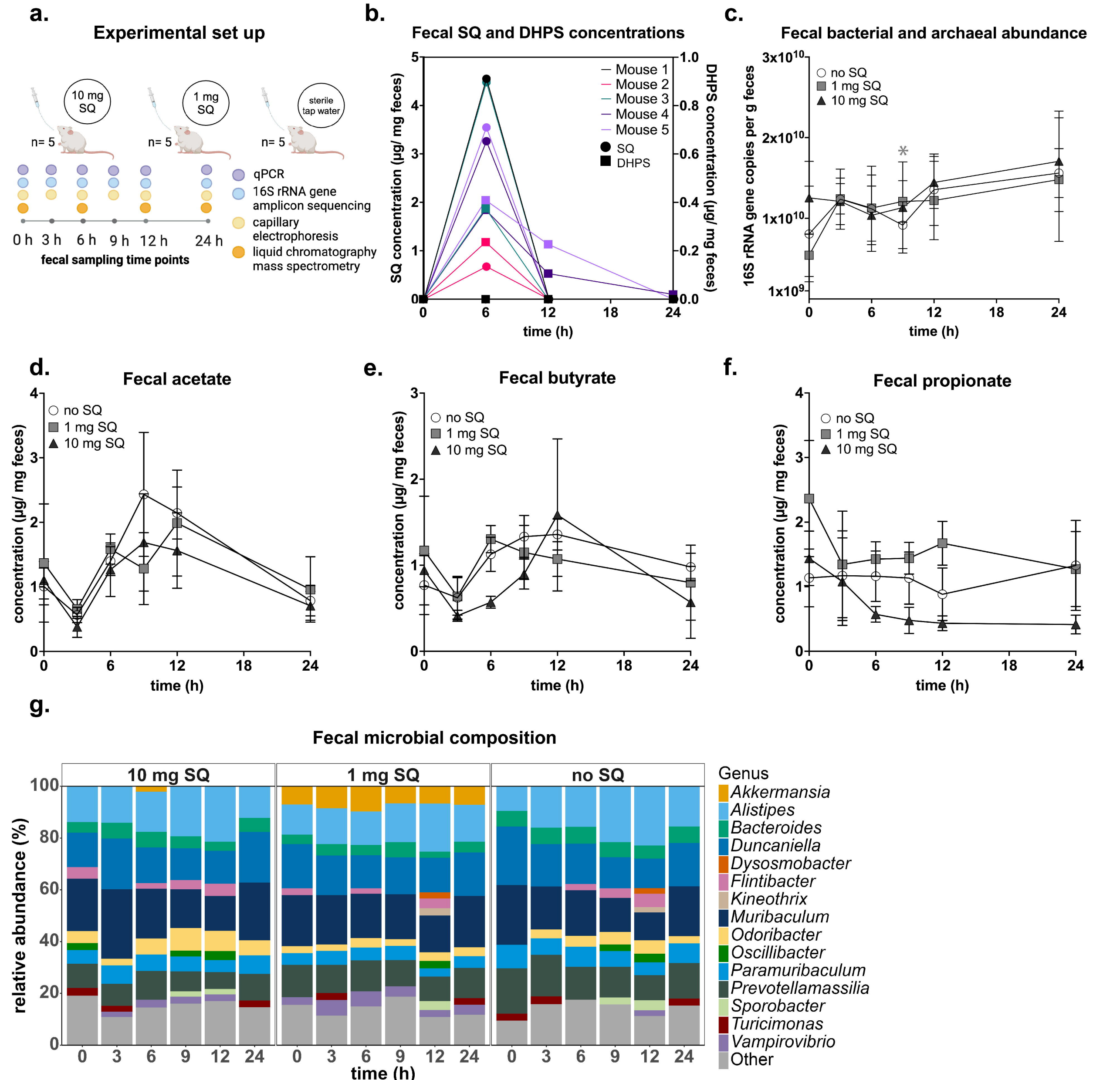
a.
Experimental set up
10 mg SQ
1 mg SQ
sterile tap water
n= 5
n= 5
n= 5
qPCR
16S rRNA gene amplicon sequencing
capillary electrophoresis
liquid chromatography mass spectrometry
0 h 3 h 6 h 9 h 12 h 24 h
fecal sampling time points
b.
Fecal SQ and DHPS concentrations
Mouse 1
Mouse 2
Mouse 3
Mouse 4
Mouse 5
SQ
DHPS
SQ concentration (µg/ mg feces)
DHPS concentration (µg/ mg feces)
time (h)
c.
Fecal bacterial and archaeal abundance
no SQ
1 mg SQ
10 mg SQ
16S rRNA gene copies per g feces
time (h)
d.
Fecal acetate
no SQ
1 mg SQ
10 mg SQ
concentration (µg/ mg feces)
time (h)
e.
Fecal butyrate
no SQ
1 mg SQ
10 mg SQ
concentration (µg/ mg feces)
time (h)
f.
Fecal propionate
no SQ
1 mg SQ
10 mg SQ
concentration (µg/ mg feces)
time (h)
g.
Fecal microbial composition
10 mg SQ
1 mg SQ
no SQ
relative abundance (%)
time (h)
Genus
Akkermansia
Alistipes
Bacteroides
Duncaniella
Dysosmobacter
Flintibacter
Kineothrix
Muribaculum
Odoribacter
Oscillibacter
Paramuribaculum
Prevotellamassilia
Sporobacter
Turicimonas
Vampirovibrio
Other

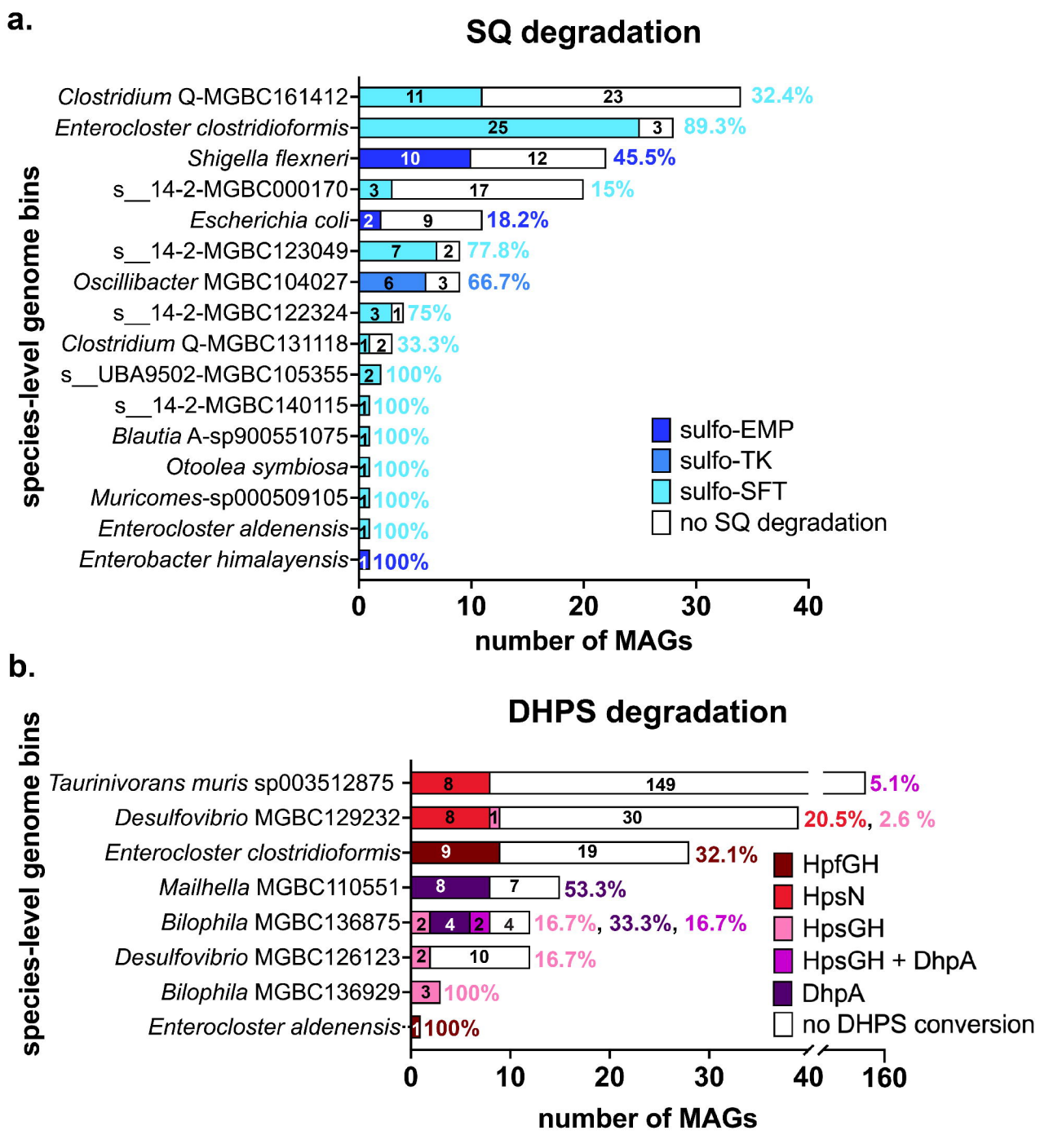
a.
SQ degradation
species-level genome bins
Clostridium Q-MGBC161412
Enterocloster clostridioformis
Shigella flexneri
s__14-2-MGBC000170
Escherichia coli
s__14-2-MGBC123049
Oscillibacter MGBC104027
s__14-2-MGBC122324
Clostridium Q-MGBC131118
s__UBA9502-MGBC105355
s__14-2-MGBC140115
Blautia A-sp900551075
Otoolea symbiosa
Muricomes-sp000509105
Enterocloster aldenensis
Enterobacter himalayensis
11
23
32.4%
25
3
89.3%
10
12
45.5%
3
17
15%
2
9
18.2%
7
2
77.8%
6
3
66.7%
3
1
75%
1
2
33.3%
2
100%
1
100%
1
100%
1
100%
1
100%
1
100%
sulfo-EMP
sulfo-TK
sulfo-SFT
no SQ degradation
0
10
20
30
40
number of MAGs
b.
DHPS degradation
species-level genome bins
Taurinivorans muris sp003512875
Desulfovibrio MGBC129232
Enterocloster clostridioformis
Mailhella MGBC110551
Bilophila MGBC136875
Desulfovibrio MGBC126123
Bilophila MGBC136929
Enterocloster aldenensis
8
149
5.1%
8
1
30
20.5%, 2.6 %
9
19
32.1%
8
7
53.3%
2
4
2
4
16.7%, 33.3%, 16.7%
2
10
16.7%
3
100%
1
100%
HpfGH
HpsN
HpsGH
HpsGH + DhpA
DhpA
no DHPS conversion
0
10
20
30
40
160
number of MAGs

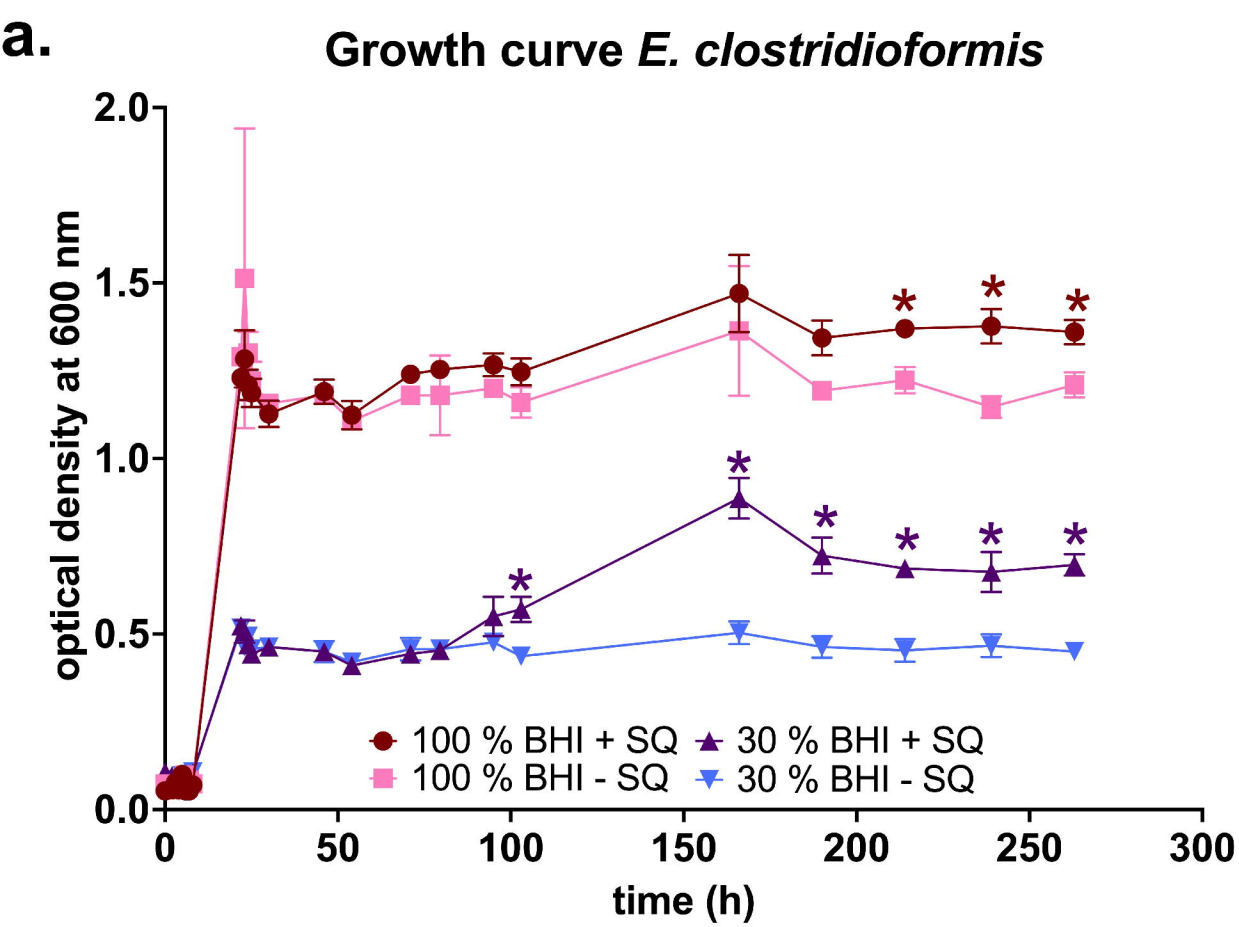
a.
Growth curve E. clostridioformis
optical density at 600 nm
time (h)
100 % BHI + SQ
100 % BHI - SQ
30 % BHI + SQ
30 % BHI - SQ

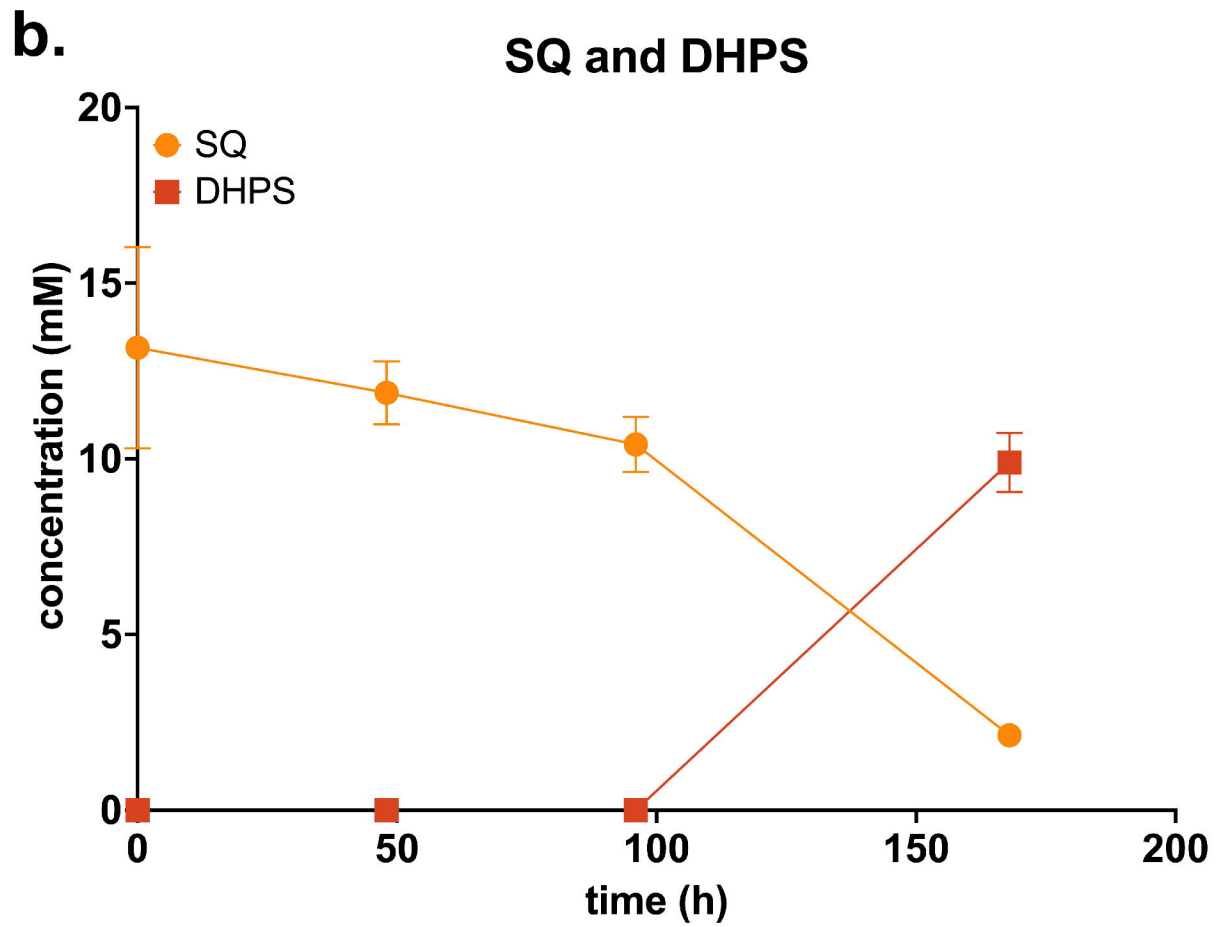
b.
SQ and DHPS
SQ
DHPS
concentration (mM)
time (h)

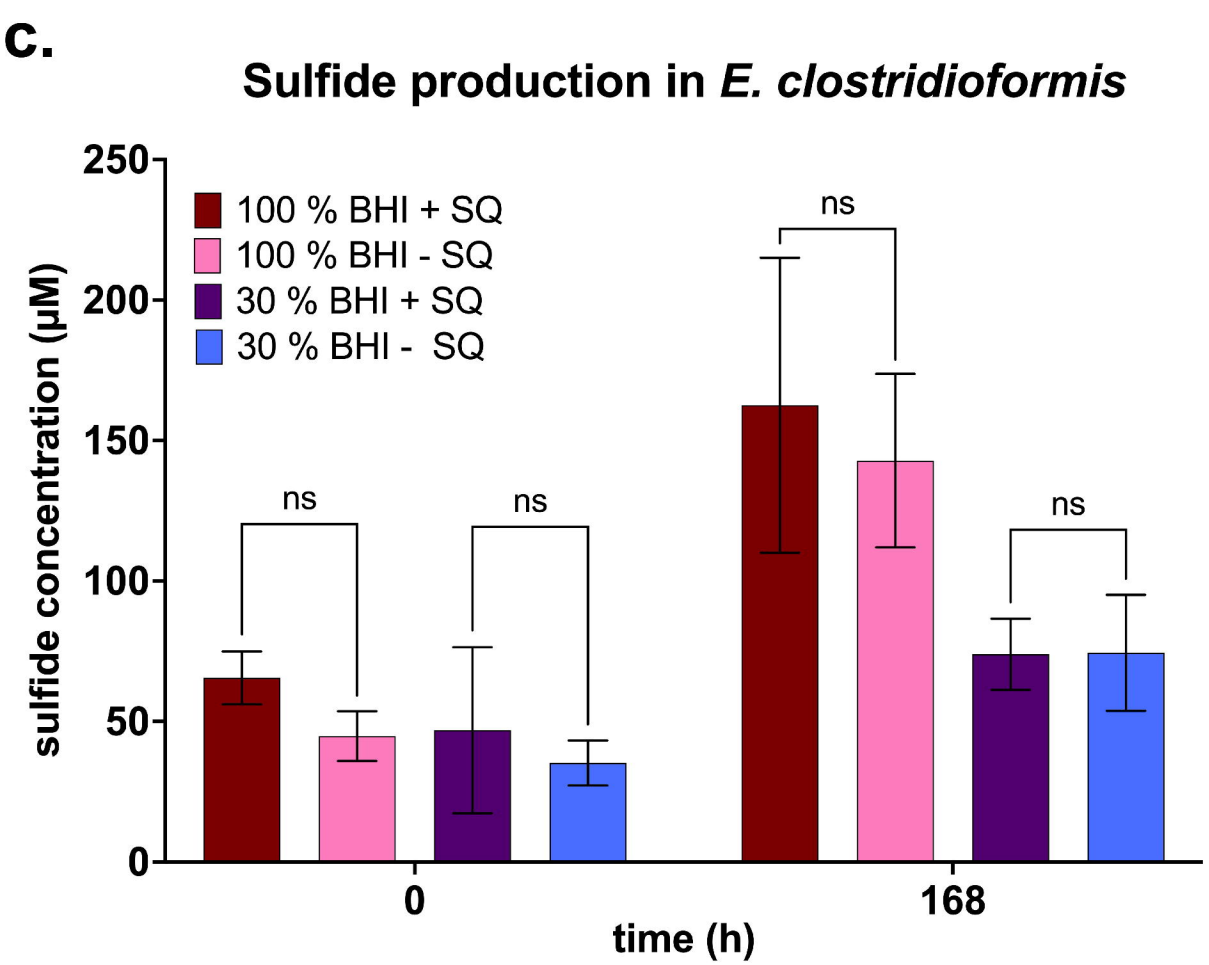
c.
Sulfide production in E. clostridioformis
100 % BHI + SQ
100 % BHI - SQ
30 % BHI + SQ
30 % BHI - SQ
ns
sulfide concentration (µM)
time (h)

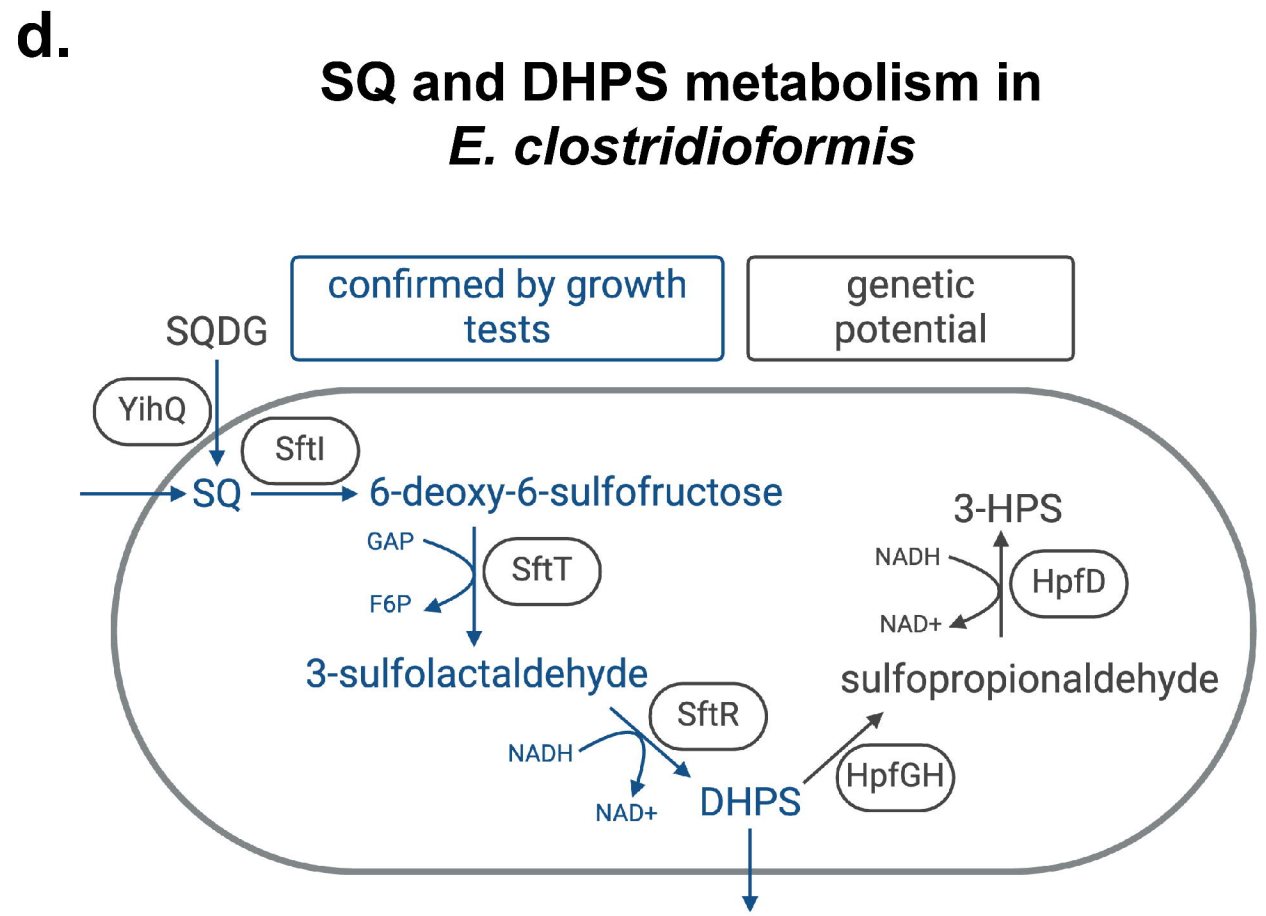
d.
SQ and DHPS metabolism in
E. clostridioformis
confirmed by growth tests
genetic potential
SQDG
YihQ
SftI
SQ
6-deoxy-6-sulfofructose
GAP
F6P
SftT
3-sulfolactaldehyde
NADH
NAD+
SftR
DHPS
HpfGH
sulfopropionaldehyde
3-HPS
NADH
NAD+
HpfD